



A new giant salamander (Urodela, Pancryptobranchia) from the Miocene of Eastern Europe (Grytsiv, Ukraine)

Davit Vasilyan , Madelaine Böhme , Viacheslav M. Chkhikvadze , Yuriy A. Semenov & Walter G. Joyce

To cite this article: Davit Vasilyan , Madelaine Böhme , Viacheslav M. Chkhikvadze , Yuriy A. Semenov & Walter G. Joyce (2013) A new giant salamander (Urodela, Pancryptobranchia) from the Miocene of Eastern Europe (Grytsiv, Ukraine), *Journal of Vertebrate Paleontology*, 33:2, 301-318, DOI: [10.1080/02724634.2013.722151](https://doi.org/10.1080/02724634.2013.722151)

To link to this article: <http://dx.doi.org/10.1080/02724634.2013.722151>



[View supplementary material](#)



Published online: 05 Mar 2013.



[Submit your article to this journal](#)



Article views: 206



[View related articles](#)



Citing articles: 5 [View citing articles](#)

A NEW GIANT SALAMANDER (URODELA, PANCRYPTOBRANCHIA) FROM THE MIOCENE OF EASTERN EUROPE (GRYTSIV, UKRAINE)

DAVIT VASILYAN,^{*1} MADELAINE BÖHME,^{1,2} VIACHESLAV M. CHKHIKVADZE,³ YURIY A. SEMENOV,⁴ and WALTER G. JOYCE¹

¹Department of Geosciences, Eberhard-Karls-University Tübingen, Sigwartstraße 10, 72076 Tübingen, Germany,
davit.vasilyan@ifg.uni-tuebingen.de; walter.joyce@uni-tuebingen.de;

²Senckenberg Center for Human Evolution and Palaeoecology, Sigwartstraße 10, 72076 Tübingen, Germany,
m.boehme@ifg.uni-tuebingen.de;

³Institute of Paleobiology, Georgian National Museum, Niagvari str. 4, 0108 Tbilisi, Georgia, chelydrasia@gmail.com;

⁴National Museum of Natural History, National Academy of Sciences of Ukraine, Bogdan Khmelnytski str. 15, 01601, Kiev,
Ukraine, yuriy_semenov@mail.ru

ABSTRACT—We present new and well-preserved giant salamander material from the Miocene of the Grytsiv locality, Ukraine. Disarticulated skull and postcranial bones from two individuals are described as a new taxon, *Ukrainurus hypsognathus*, gen. et sp. nov. *U. hypsognathus* is characterized by poorly ossified bone tissues, relatively inflexible mandibles, a high dentary, a crista on the lingual surface of the dentary, a pars dentalis of the dentary that is composed of a dental lamina and a subdental surface, presence of an eminentia dorsalis on the squamosal, a broad pericondylar facet on the occipital, extremely elongated prezygapophyses, and hemal processes with an elongate, oval base. Moreover, *U. hypsognathus* shows evidence of strong mandibular levator muscles that indicate great biting force. A phylogenetic analysis of all well-understood Tertiary and Recent giant salamanders recovers a monophyletic group of Asian and North American cryptobranchids, but places *U. hypsognathus* outside crown group Cryptobranchidae. This result suggests that Cryptobranchidae originated in Asia and dispersed to North America. The oldest representative of crown Cryptobranchidae is *Aviturus exsecratus* from the terminal Paleocene of the Nemegt Basin, Mongolia.

SUPPLEMENTAL DATA—Supplemental materials are available for this article for free at www.tandfonline.com/UJVP

INTRODUCTION

Cryptobranchids (giant salamanders) represent a clade of large salamanders that can reach over 1.5 m in total length. They are strictly aquatic amphibians that are today confined to clear, well-oxygenated, cold mountain streams and rivers (Vitt and Caldwell, 2009). Twelve species ranging throughout the Tertiary are currently referred to Cryptobranchidae (Westphal, 1958; Chkhikvadze, 1982; Gubin, 1991; Böhme and Ilg, 2003; Gao and Shubin, 2003; Holman, 2006), but the taxonomic validity of some taxa (e.g., *Ulanurus fractus* Gubin, 1991) is unclear and their phylogenetic affinities are poorly understood. Three poorly understood taxa from the Mesozoic of Asia (*Chunerpeton tianyiensis* Gao and Shubin, 2003, *Eoscaphepon asiaticum* Nesson, 1981, and *Horezmia gracilis* Nesson, 1981) have also been referred to Cryptobranchidae, but it is clear that these animals are representatives of the cryptobranchid stem lineage at best (see Discussion). In the fossil record, cryptobranchids are particularly well represented in the Cenozoic of Eurasia and at least 56 fossil localities are currently known (Böhme and Ilg, 2003). All Neogene Eurasian fossils have been attributed to the Recent genus *Andrias*, but only one species, *Andrias scheuchzeri* (Holl, 1831), is well documented (Westphal, 1958). The majority of occurrences are from Central Europe and little is known about cryptobranchids from Eastern Europe. Here we describe a considerable collection of bones of two giant salamander individuals collected by Y. A. Semenov and W. M. Chkhikvadze from the Ukrainian

locality Grytsiv. The larger individual was collected during the 1987 field season, the smaller individual during the 1988 field season. The purpose of this contribution is to describe the new material as a new taxon and to analyze, for the first time, the phylogenetic relationships of fossil and Recent giant salamanders.

GEOLOGICAL OVERVIEW

The Grytsiv locality (Fig. 1) is situated in the western part of Ukraine (Shepetovka Rayon), 240 km west of Kiev. The outcrop represents an abandoned limestone quarry along the Khoroma River, 1.5–2 km west of the village of Grytsiv (coordinates: 49.96°N, 27.21°E). The section is up to 12 m thick and comprises a sequence of greenish silts and biogenic algal reef carbonates, situated over a granitic basement (Korotkevich et al., 1985; Topachevskij et al., 1996). Both marine facies contain an early Bessarabian mollusk fauna, including *Sarmatimactra vitaliana*, *Venerupis ponderosus*, and *Obsoletiforma obsoleta vindobonensis* (Korotkevich et al., 1985; Korotkevich, 1988). These sediments represent one of the northernmost outcrops of the early Bessarabian transgression (Novomoskovsky horizon of Didkovsky, 1964) onto the Ukrainian shield (Pevzner and Vangengeim, 1993). The carbonates are overlain in this region by greenish clays that contain the same early Bessarabian mollusk fauna. These clays are also preserved in karst fissures and holes within the reef carbonate, indicating their formation under terrestrial conditions during a sea-level lowstand. The greenish clays contain an exceptionally well preserved, rich, and diverse vertebrate assemblage, including partial skeletons. On top of

*Corresponding author.

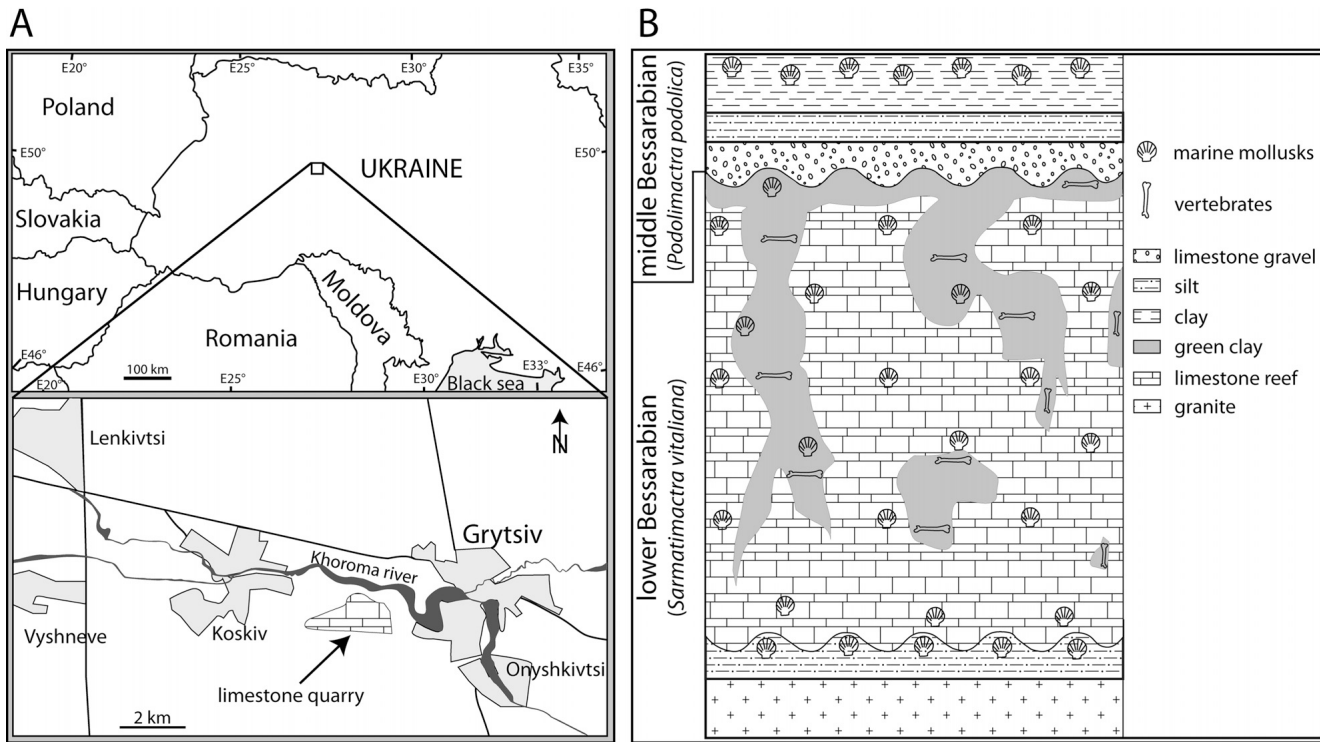


FIGURE 1. A, map of Ukraine showing the location of the limestone quarry near Grytsiv; B, geological profile at Grytsiv, redrawn from Korotkevich (1988) and Topachevskij et al. (1996).

this level follows a transgressive horizon composed of reworked carbonates, which, in return, is succeeded by more clays and siltstones indicating the next sea-level highstand. The mollusk fauna of this second cycle contain *Podolimactra podolica*, indicative of a middle to late Bessarabian age (Topachevskij et al., 1996).

The sediments that contain the vertebrate fauna are confined to the latest part of the early Bessarabian (*Sarmatimactra vitaliana pallasi* interval zone of Kojumdgieva et al., 1989) near the early-middle Bessarabian boundary. Based on mollusks, the early Bassarabian of the Eastern Paratethys can be correlated to the late Sarmatian of the Central Paratethys (Rögl, 1998; Harzhauser and Piller, 2004), which in return correlates to the late Serravallian (latest middle Miocene). The reverse magnetic polarity of the greenish clay (Chepalyga et al., 1985) furthermore enables a correlation with magnetic chron C5r (12.014 to 11.040 Ma according to Lourens et al., 2004). This agrees with an early Vallesian biostratigraphic age of the fauna, characterized by the first appearance date of the horse *Hippotherium* (in Grytsiv with *H. primigenium* and *H. sp.*; Krakhmalnaya, 1996). The Grytsiv fauna is older than the Moldovan faunas of Kalfa and Buzhor 1 (Nesin and Nadachowski, 2001; contra Vangengeim et al., 2006), which both contain late middle Bessarabian sediments (Vasilievsky horizon of Didkovsky, 1964; below and within horizons with *Plicatiforma fittoni*, *Podolimactra podolica*, and *Sarmatimactra fabreana*; Roshka, 1967; Lungu, 1978, 1981) that correspond to the lower part of the *Plicatiformis fittoni fittoni* range zone of Kojumdgieva et al. (1989).

MATERIALS AND METHODS

The bones of each specimen (a large one and a small one) of *Ukrainurus hypsognathus* described here were found in two separate fossiliferous pockets. In each batch, bones are from animals of comparable size and the bones do not duplicate each other.

However, because the bones were not found articulated, we prefer to erect the new species based on the left dentary only.

All Grytsiv fossils are deposited in the National Museum of Natural History (National Academy of Sciences), Kiev, Ukraine. For comparison, the following specimens of Recent cryptobranchoids were considered: *Andrias japonicus* (Temminck, 1836) (NMA, unnumbered specimen; SMNS 7898:1–15; ZIT 240; ZMB 9928), *Andrias davidianus* (Blanchard, 1871) (SMF 89293; ZFMK 76996, 90469), *Andrias* sp. (SMF 69133), *Cryptobranchus alleganiensis* (Daudin, 1803) (ZFMK 5245; SMNK 201; SMNK uncataloged), and *Onychodactylus fischeri* (Bouleenger, 1886) (GPIT/RE/7331). Our observations of the fossil taxon *Andrias scheuchzeri* from the North Alpine Foreland Basin of Europe are based on NMA-2009-1/2076-11/2076, NMA-2009-26/2076, NMA-2010-221/2076-232/2050, NMA-2/2076, NMA-346/1633, SMNS 55314, GPIT/AM/717, CGPUJ 201.104, CGPUJ 201.105, SMNPAL.6612-6618, PIMUZ A II 1, and PIMUZ A II 2; those of *Zaissanurus beliajevae* Chernov, 1959, from the Paleogene of the Zaisan Basin are based on PIN 416-1, IP ZSN-KKS-2, IP ZSN-K-11, IP ZSN-K-14, IP ZSN-K-15, IP ZSN-Y-9; those of *Ulanurus fractus* from the Paleogene of the Nemegt Basin are based on PIN 4357/27 and PIN 4358/2; and those of *Salamandrella* sp. from the late Miocene of Ertemte 2, China, are based on an unnumbered GPIT specimen. Our observations on *Aviturus exsecratus* Gubin, 1991, from the Paleogene of the Nemegt Basin are based on the description of Gubin (1991) and those of '*Cryptobranchus*' *saskatchewanensis* (Naylor, 1981) are based on the description of Naylor (1981). Because we were not able to observe relevant material of '*C.*' *saskatchewanensis* in person, we regard the generic identity of this species as uncertain.

The terminology used to describe the individual bones and their features is based, where possible, on Osawa (1902), Francis (1934), Cundall et al. (1987), Duellman and Trueb (1994), Elwood and Cundall (1994), Gardner (2003), and Skutschas

(2009). The nomenclature of muscles follows that of Elwood and Cundall (1994).

Dentary cross-sections of *Ukrainurus hypsognathus*, gen. et sp. nov., *An. scheuchzeri*, and *An. davidianus* were made using a Siemens X-ray computer tomography (CT) scanner at the Department of Radiology of the University of Tübingen, Germany. Natural cross-sections of *Z. beliaejevae* were drawn using the software Adobe Illustrator. Bone compactness was estimated using the software program Bone Profiler 2010 (Girondot and Laurin, 2003).

Cross-sections of the dentary were studied at the following positions: (1) at the narrowest point between the symphysis and the Meckelian groove; (2) behind the beginning of the Meckelian groove; (3) halfway between the anterior limit of the Meckelian groove and the posterior end of the dental lamina; and (4) at the posterior-most part of the dental lamina.

Institutional Abbreviations—**CGPUJ**, Collection Geology and Palaeontology, Universalmuseum Joanneum, Graz, Austria; **GPIT**, Institut für Geowissenschaften, Universität Tübingen, Tübingen, Germany; **IP**, Institute of Paleobiology, National Museum of Georgia, Tbilisi, Georgia; **NHMUK**, Department of Zoology, Natural History Museum, London, U.K.; **NMA**, Naturmuseum Augsburg, Augsburg, Germany; **NMNHK**, National Museum of Natural History, Kiev, Ukraine; **PIMUZ**, Paläontologisches Institut und Museum der Universität Zürich, Zurich, Switzerland; **PIN**, Paleontological Institute, Russian Academy of Sciences, Moscow, Russia; **SMF**, Senckenberg Naturmuseum, Frankfurt am Main, Germany; **SMNK**, Staatliches Museum für Naturkunde, Karlsruhe, Germany; **SMNS**, Staatliches Museum für Naturkunde, Stuttgart, Germany; **ZFMK**, Zoologisches Forschungsmuseum Koenig, Bonn, Germany; **ZIT**, Institute of Zoology, University of Tübingen, Tübingen, Germany.

SYSTEMATIC PALEONTOLOGY

AMPHIBIA Linnaeus, 1758

LISSAMPHIBIA Haeckel, 1866

CAUDATA Scopoli, 1777

PANCRIPTOBRANCHIA, clade nov.

Diagnosis—Representatives of Pancryptobranchia can be diagnosed by (numbers in parentheses refer to the character matrix used herein): the presence of unicapitate trunk ribs (32); large body size (33); and a contact between the parietal and the squamosal (34).

Currently Hypothesized Content—Pancryptobranchia is currently hypothesized to include *Ukrainurus hypsognathus*, sp. nov., and Cryptobranchidae.

Comments—Our phylogenetic analysis (see below) reveals that the new fossil taxon is sister to the clade formed by extant cryptobranchids and we therefore must distinguish between total group (stem group) and crown group Cryptobranchidae. We herein follow the wide spread convention (Joyce et al., 2004) and use the historical term ‘Cryptobranchidae’ to refer to the crown group and coin the new term Pancryptobranchia for the total group.

UKRAINURUS, gen. nov.

Type Species—*Ukrainurus hypsognathus*, sp. nov.

Diagnosis—Same as for the type species.

Etymology—The generic name alludes to the country of origin (Ukraine) and ‘-urus’ (*οὐρά*), Greek for tail.

UKRAINURUS HYPSOGNATHUS, sp. nov.

(Figs. 2–8)

Holotype—NMNHK 22-1711, a left dentary.

Paratypes—All bones assigned to the larger of the two available individuals: left and right articulars (NMNHK 22-1711ar-a and NMNHK 22-1711ar-b); right coronoid (NMNHK

22-1711c); left and right squamosals (NMNHK 22-1711sq-a and NMNHK 22-1711sq-b); left and right quadrates (NMNHK 22-1711q-a and NMNHK 22-1711q-b); left orbitosphenoid (NMNHK 22-1711os); left occipital (NMNHK 22-1711oc); right femur (NMNHK 22-1707); six ribs (NMNHK 22-1707a); two terminal phalanges (NMNHK 22-1711f); and six trunk vertebrae (NMNHK 22-1698, NMNHK 22-1699, NMNHK 22-1704, NMNHK 22-1705, NMNHK 22-1706, NMNHK 22-1706a). The smaller of the two available individuals, consisting of nine trunk vertebrae (NMNHK 22-1706b, NMNHK 22-1706c, NMNHK 22-1706d, NMNHK 22-1706-88a, NMNHK 22-1706-88b, NMNHK 22-1706-88c, NMNHK 22-1706-88d, NMNHK 22-1706-88e, NMNHK 22-1706-88f); a pterygapophysis (NMNHK 22-1706f); and one caudal vertebra (NMNHK 22-1706e).

Type Locality—An abandoned quarry 1.5–2 km southeast of the village of Grytsiv (also Gritsev), Shepetivskyi Rayon, Ukraine.

Type Horizon—Karstic fissure fills in early Bessarabian reef limestones.

Stratigraphy—Middle to late Miocene transition (early to late Bessarabian transition), magnetochron C5r, mammal ‘zone’ MN9 (Topachevskij et al., 1996).

Diagnosis—The new taxon can be diagnosed as a representative of Pancryptobranchia based on the following list of characters (numbers in parentheses refer to the character matrix used herein): trunk ribs unicapitate (32); body size large (33); and parietal and squamosal in contact with one another (34). The following list of characters are unambiguous apomorphies of the new taxon within Pancryptobranchia: symphysis elongated and elliptical (1); triangular ventral space between the dentaries is small (2); sculpture of the dermal ossification on labial side of dentary is rugose to pustular and pointed (3); lingual crista on dentary present (4); ventral keel prolonged (6); pars dentalis subdivided into a dental and subdental lamina (7); mental foramina large, longitudinal flange pronounced (9); labioventral facet of articular broad and sculptured with highly prominent pits and ridges (14); pericondyilar facet of occipital broad (19); squamosal robust (20); eminentia dorsalis present (21); paries posterior high (22); paries posterior runs along paries dorsal with an obtuse angle (23); beginning of hemal process oval (27); hemal processes positioned at the posterior portion of vertebral centrum (28); arterial canal in caudal vertebrae broad, with large foramen (29); terminal phalanges slender, with bulbous tips (30); and degree of ossification of the dentary low (bone compactness value >0.8) (31). The new taxon is furthermore diagnosed by one ambiguous apomorphy, which is homoplastic with *Andrias scheuchzeri*: coronoid process broad (17).

Etymology—The specific name derives from a characteristic feature of this animal, its high dentary: in Greek ‘*hypso*’ (*υψηλός*), high, and ‘-gnathos’ (*γνάθος*), jaw bone.

DESCRIPTION

Skull

Dentary—The dentary (NMNHK 22-1711) is long, high, and strongly compressed labiolingually (Fig. 2). The length of the dentary is 110.8 mm between the posterior and anterior tips and 121.25 mm along the labial surface. The height of the dentary near the symphysis is 21.2 mm. The posteroventral half of the bone, under the Meckelian groove, is absent. The depth of the pars dentalis is less than half of the depth of the corpus dentalis.

The symphysis is not well preserved; only the labial part is present. From what is available, we nevertheless speculate that it was elliptical in outline. The symphyseal surfaces are almost smooth along their margins but become rugose towards their center. The (inter)mandibular joint is formed by the posterior part of the symphysis. The posterior part slopes ventrolaterally

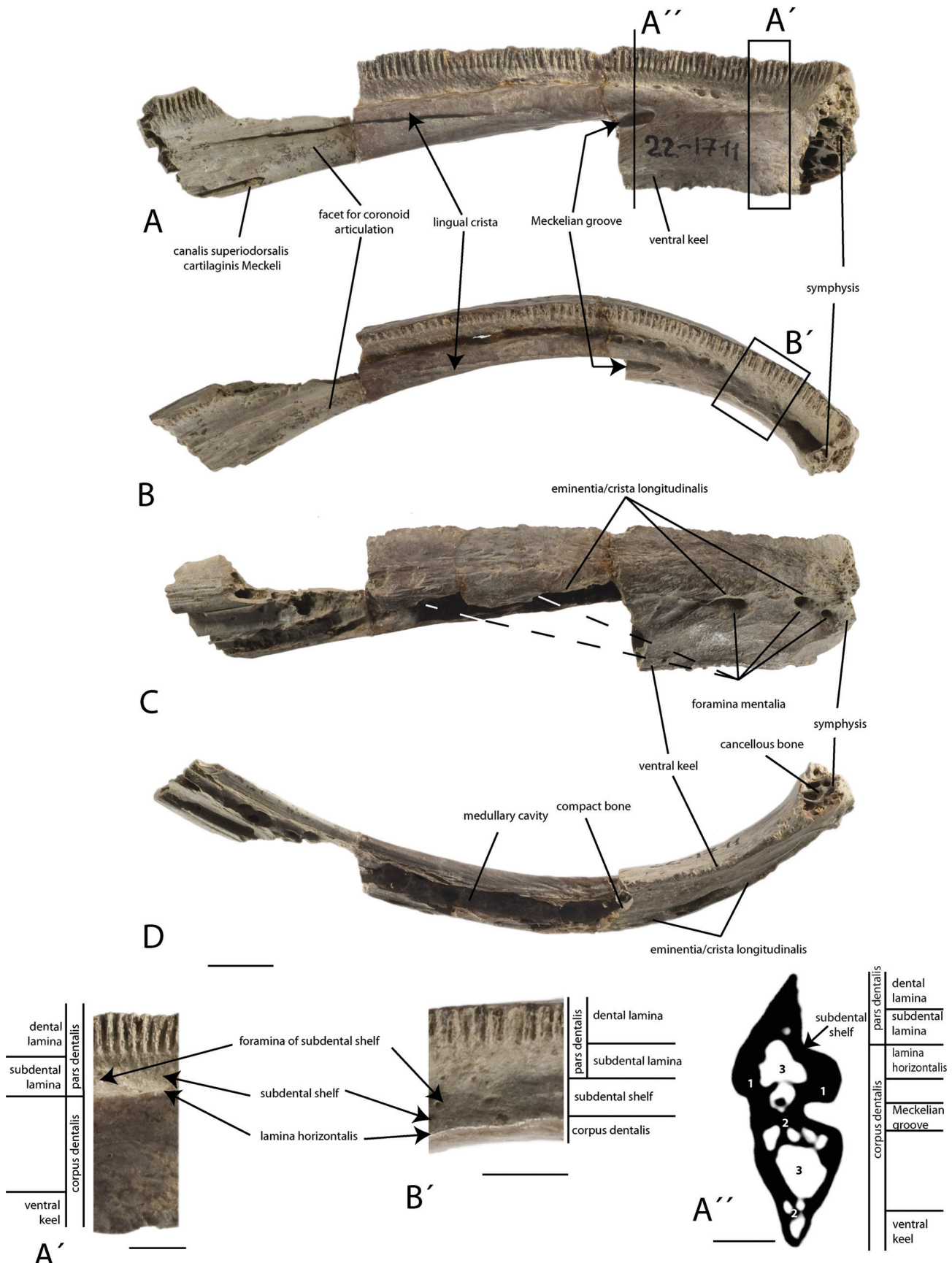


FIGURE 2. Dentary (NMNHK 22-1711) of *Ukrainurus hypsognathus*, gen. et sp. nov. **A**, **A'**, lingual views, **A''**, cross-section behind the anterior limit of the Meckelian groove made by CT [**1**, cortical and **2**, cancellous bones; **3**, medullary cavity]; **B**, **B'**, dorsal, **C**, labial (mirrored), and **D**, ventral views. Scale bars equal 1 cm (**A–D**) and 5 mm (**A'**, **B'**, **A''**). (Color figure available online.)

and provides space for the ventral symphyseal cartilage (Cundall et al., 1987).

In lingual view, the pars dentalis lies above the subdental shelf (sulcus dentalis sensu Meszoely, 1966; dental gutter sensu Naylor, 1981) and is composed of dental and subdental laminae of relatively equal depth that are arranged parallel to each other (Fig. 2A). Pedicels of pleurodont teeth are visible along the dental laminae. The surface of the subdental lamina is almost smooth, but slightly pronounced subvertical lines are nevertheless apparent (Fig. 2A, A').

The dental and subdental laminae are high and narrow near the symphysis, decrease in height and increase in thickness in the middle part, but posteriorly increase in height again. The pars dentalis is nearly twice as high as the dental lamina near the symphysis, 1.2 times in the middle portion of the dentary, and 2.2 times at the posterior-most part of dentary. In the anterior part of the dentary, the pars dentalis is less than half as long as the corpus dentalis (Fig. 2A, A', B').

The dentition on the dentary is monostichous. The tooth crowns are missing and the teeth are therefore represented by their pedicellar portions only. The pedicels indicate that the teeth are narrow and numerous. At least 110 teeth must have been present. The dental lamina is 115 mm long.

The subdental shelf is flat in the anterior and posterior portions, but shallow in the middle part. The surface exhibits irregularly placed small foramina and larger pits, which might be piercing the compact bone and connecting the external surface with the medullary cavity (Fig. 3Bi). The anterior-most foramen is the largest and connects with the symphysis.

The anterior part of the dental shelf is broad and accentuated. The margin of the lamina horizontalis is angular. Above the anterior tip of the Meckelian groove, the dental shelf exhibits a marked step, decreasing in width by around 50%, and the ridge of the lamina horizontalis becomes rounded. Posterior to this point, the lamina is angular again (Fig. 2A, B). The anterior portion of the Meckelian groove is deep and narrow and extends 3 mm into the bone. The posterosuperior margin of the Meckelian groove is pierced by a canal (canalis superperiodorsalis cartilagineus Meckelii) for the nervus alveolaris und arteria temporalis (sensu Böttcher, 1987). This canal extends 12 mm into the bone (Fig. 2A).

The lingual surface of the corpus dentalis (subdental shelf sensu Gardner and Averianov, 1998) is smooth. Only some small foramina are present. In transverse section, the corpus dentalis is broad superiorly, narrows inferiorly, and ends with a ventral keel. The keel margin is characterized by sparse pustules/warts (Fig. 2A, C, D). The articulation facet with the coronoid on the lingual side of dentary, above the Meckelian groove, forms a sharp lingual crista, which extends subparallel to the inferior margin of dental lamina and fuses posteriorly with the lamina horizontalis (Fig. 2A, B).

The longitudinal axis of the dentary separates the pars dentalis from the corpus dentalis. A longitudinal flange (eminencia longitudinalis) extends labially from this axis. The sculpture of the perichondral ossification on the labial side of the dentary is rugose to pustular. These surface structures are more pronounced directly behind the symphysis and on the ventral margin of the longitudinal flange, which overlies the mental foramina. Two grooves are furthermore present that extend to the center of the symphysis in the labioanterior part of dentary. The superficial symphyseal ligament of the mandibular joint attached at this site (Cundall et al., 1987). Five mental foramina are arranged on the labial side of the dentary along the longitudinal axis. There are also some small foramina on the labial side of the pars dentalis.

Like all of the other bones, the dentary is weakly ossified. It has an extremely thin cortex that surrounds cancellous bone. The medullary cavity is extensive (Figs. 2A'', 3B). In cross-section,

TABLE 1. Bone density values of studied giant salamander dentaries at the given positions (see Fig. 3).

Taxon	n	Value			
		i	ii	iii	iv
<i>Zaissanurus beliaevae</i> (IP ZSN-KKS-2)	1	0.837	0.808	?	?
<i>Ukrainurus hypsognathus</i> (NMNHK 22-1711)	1	0.721	0.603	?	?
<i>Andrias scheuchzeri</i> (GPIT/AM/717)	1	0.893	0.728	0.755	0.83

two large medullary cavities are apparent dorsal and ventral to the longitudinal flange. Smaller cavities are arranged around these primary cavities. The ventral keel encloses small medullary cavities, which are present in the anterior portion of the dentary. The total medullary cavity of the dentary is not a closed system fully surrounded by bone. Instead, the cavity communicates with the outside via numerous mental foramina, the anterior part of the Meckelian groove, and small foramina along the dental shelf. The medullary cavities extend posteriorly where the two main cavities diffuse into compact bone (Fig. 3). The bone compactness values of the available cross-sections are given in Table 1. There is a general trend in that bone compactness values changes along the dentary. In particular, bone compactness values are comparably higher anteriorly and posteriorly, but lower in the midsection (see Table 1).

Articular—The articular (angular sensu Osawa, 1902; Reese, 1906; Duellman and Trueb, 1994) is a long, straight, and slender bone. Anteriorly, it narrows and its walls thin (Fig. 4). The posterior end of the articular is massive; on the dorsal side it bears a rounded, slightly elliptical articular condyle (pars condyloidea cartilaginea sensu Hyrtl, 1885). This is the mineralized/ossified posterior portion of the Meckelian cartilage (Buckley et al., 2010).

Much of the labial surface of the articular covers the dentary. The transition between these two bones, however, is nearly invisible. The linguoventral side of the articular has a broad facet (facies coronoideus; Fig. 4A, B) with a highly prominent pit-and-ridge sculpture that narrows anteriorly. The articular covers the articular facet of the coronoid with this facet. Posteriorly, the articular ends with a ventroposteriorly extended elliptical surface, which bears two small pits (Fig. 4A). The posterior fibers of the mandibular depressor muscles attached to this surface.

Coronoid—The flat, wedge-shaped coronoid (prearticular sensu Duellman and Trueb, 1994) lacks its anterior and posterior parts. Labially, the bone is concave and covers the lingual side of the Meckelian cartilage. The bone has a relatively smooth surface. Only the articular and dental facets, dorsal edge of the lingual surface, and the dorsal coronoid process are bumpy to wrinkled. The bone is high at the anterior-most part of the coronoid process and slender posteriorly and anteriorly (Fig. 4). In the middle part, the coronoid ascends dorsoligually to form a fairly pronounced and flattened coronoid process. This large and long process is nearly triangular in dorsal view, wing-like, and protrudes over the lingual surface of the bone. The dental facet of the coronoid starts at the lingual corner of the coronoid process and extends anteroventrally. The preserved part of articular facet is narrow (Fig. 4).

Squamosal—The squamosal (terminology by Delfino et al., 2009) is relatively robust and flattened. The bone consists of two parts: the nearly rectangular caput squamosa and the laterally directed quadrate ramus (Fig. 5B, D). As preserved, the latter part is 2 times longer than the former part. The anterior (zygomatic) and posterior (otic) processes of the squamosal are present. The otic process is about half as long as the zygomatic process. Its

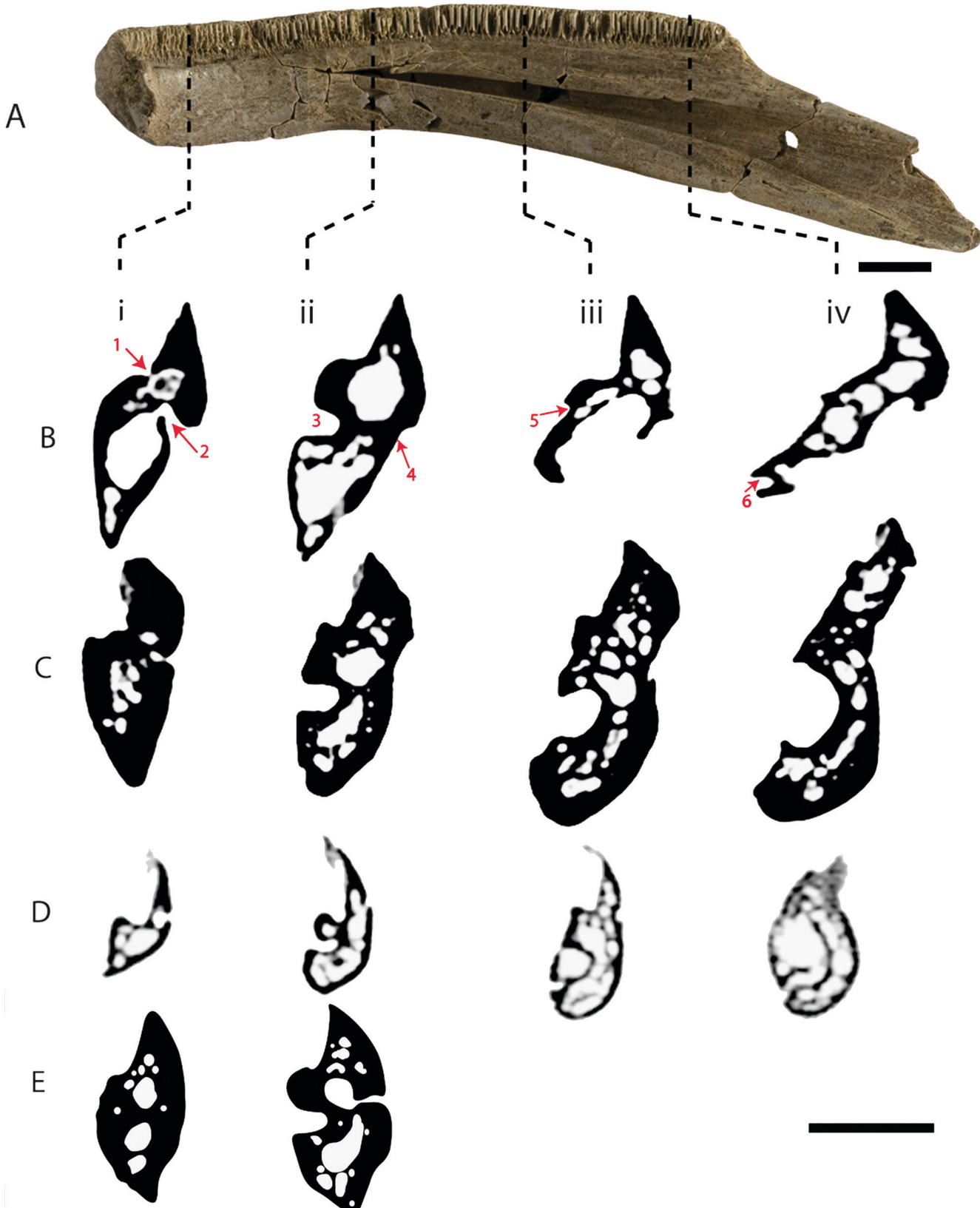


FIGURE 3. Dentary cross-sections of **A**, general view of *Andrias scheuchzeri* dentary (GPIT/AM/717) from the lingual side with the positions of cross-sections; cross-sections of **B**, *Ukrainurus hypsognathus*, gen. et sp. nov. (NMNHK 22-1711); **C**, *An. scheuchzeri* (GPIT/AM/717); **D**, *Andrias davidianus* (ZFMK 90469); and **E**, *Zaissanurus belajevae* (IP ZSN-KKS-2). **B**, **C**, **D**, were made using CT; **E**, was drawn directly from bones. Cross-section positions: **i**, between symphysis and Meckelian groove; **ii**, behind the beginning of the Meckelian groove; **iii**, in the middle part of the tooth row; **iv**, in the posterior-most part of tooth row. **1**, foramen of the dental shelf; **2**, mental foramen; **3**, Meckelian groove; **4**, eminentia longitudinalis; **5**, labial crista; **6**, canalis superiodorsalis cartilaginis Meckelii. Scale bar equals 1 cm. (Color figure available online.)

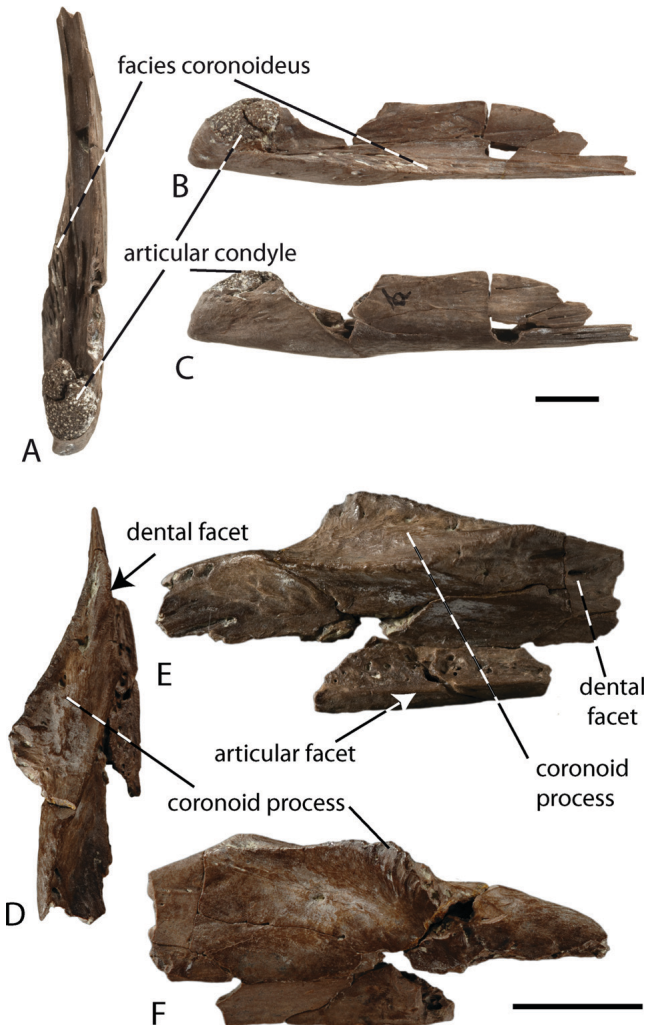


FIGURE 4. Articular and coronoid of *Ukrainurus hypsognathus*, gen. et sp. nov. Articular in **A**, dorsal, **B**, lingual, and **C**, labial views (NMNHK 22-1711a-a) and coronoid in **D**, labial, **E**, dorsal, and **F**, lingual views (NMNHK 22-1711c). Scale bars equal 1 cm. (Color figure available online.)

ventral surface is robust and directed anterolaterally (Fig. 5A, C). The otic process connects the squamosal with the prootic. The zygomatic process is pointed and directed posteriorly. Its medial surface is robust and the lateral surface is smooth. The medial ridge, ventral surface of the caput squamosa, and the zygomatic process cover the posterolateral part of the parietal.

The dorsal surface of the caput squamosa is almost smooth and exhibits some foramina. There is an anteromedially extending transverse ridge. The ridge begins at the posterodorsal edge of the medial part of the quadrate ramus and ends with an eminence (eminentia dorsalis) near the center of the caput squamosa. The dorsal margin of the caput squamosa ascends slightly and forms a highly robust, pustular surface on the medial side of the bone. The medial portion of the ventral surface of the caput squamosa is robust and bears highly prominent structures (Fig. 5B, E).

The quadrate ramus is ‘C’-shaped in anterolateral view. It is composed of three walls (paries): the paries dorsalis, which broadens anteriorly, the paries posterior, which widens laterally, and the paries ventralis, which narrows laterally (Fig. 5). The paries dorsalis and paries posterior overlie the dorsal surface

of the squamosal ramus of the quadrate. The proximal portion of the paries ventralis/pterygoideus is broader than the distal portion. This paries covers the ramus posterior of the pterygoid. In the medial part of the quadrate ramus, the paries dorsalis, and paries posterior form a right angle. Laterally, the paries posterior extends ventroposteriorly and the angle becomes obtuse. These paries probably do not form laterally a horizontal bony shelf, as can be seen in extant taxa.

Occipital—The posterior portion of the left occipital is preserved. The occipital bone produces a posterolaterally projecting, horizontally elongated occipital condyle. The facet for the odontoid process of the atlas is not preserved. The external foramen of the jugular canal is situated laterally in the middle part of the bone (foramen postoticum sensu Osawa, 1902, and Francis, 1934; foramen jugulare sensu Delfino et al., 2009). The glossopharyngeus and vagus nerves (Osawa, 1902; Francis, 1934) pass through this canal. On the dorsolateral side of the occipital, a small foramen is preserved for the spinooccipital nerve (Fig. 5F–I). The posterior part of the occipital has a slender ridge that extends subparallel to the margins of the occipital condyle. This ridge builds a pericondylar facet, which is narrow laterally and broadens dorsally and ventrally. The fibers of various neck muscles most likely inserted here (Francis, 1934).

Quadrata—The quadrates are small bones that form almost the entire articulation surface for the lower jaw. Each quadrate is a small, triangular bone that lies at the distal end of the squamosal and is largely covered by it in lateral view. The heavy, basal portion of the quadrate (quadrate caput) projects beyond the ventral margin of the squamosal. The laterodorsal surface of the quadrate caput bears the quadrate condyle, which forms the area mandibularis articularis. The slender squamosal ramus projects laterally, and lies anterior and ventral to the squamosal and dorsal to the pterygoid. In dorsal view, the squamosal ramus forms a prominence (tuber dorsale) (Fig. 5J–L).

Orbitosphenoid—The medial part of the left orbitosphenoid is preserved, but it is fragmentary and bears no morphological information.

Vertebrae

Trunk Vertebrae—The vertebrae belong to two individuals, one of which is relatively small and the other is relatively large. The vertebrae are large and massive, but all are nevertheless partly damaged. The centrum of the largest available specimen (NMNHK 22-1705) measures 32.0 mm in length, that of the smallest (NMNHK 22-1706b) 18.3 mm. The centrum is convex and dumbbell-shaped in lateral view. It is narrow in the middle part, widens towards the cotyles, and forms pericotylar crests along the margins of the cotyles. In all specimens, the centra are deeply amphicoelous and circular and subcircular in cross-section and transverse section, respectively. The central foramen is located dorsally (Fig. 6). The cotyles have a porous surface. The transverse process nearly covers the middle part of the subcentral ridge on the dorsal surface and thereby divides the ridge into the anterior and posterior alar processes (Fig. 6).

The subcentral surface of the centrum is rough and pierced by many smaller and several larger foramina. A single central foramen generally penetrates the bony tissue of the centrum from the ventral side. An additional pair of foramina is positioned lateral to the central one. Shallow and deep anteroposterior grooves adorn the interior surface of the central foramina. In addition to these foramina, the surface of the centrum is pierced by another pair of foramina (ventral foramina for spinal nerve) that are positioned under the ventral wall of the transverse processes in the subcentral groove (Fig. 6).

The neural canal is depressed and wide. Two small processes are situated near the center of the centrum and extend

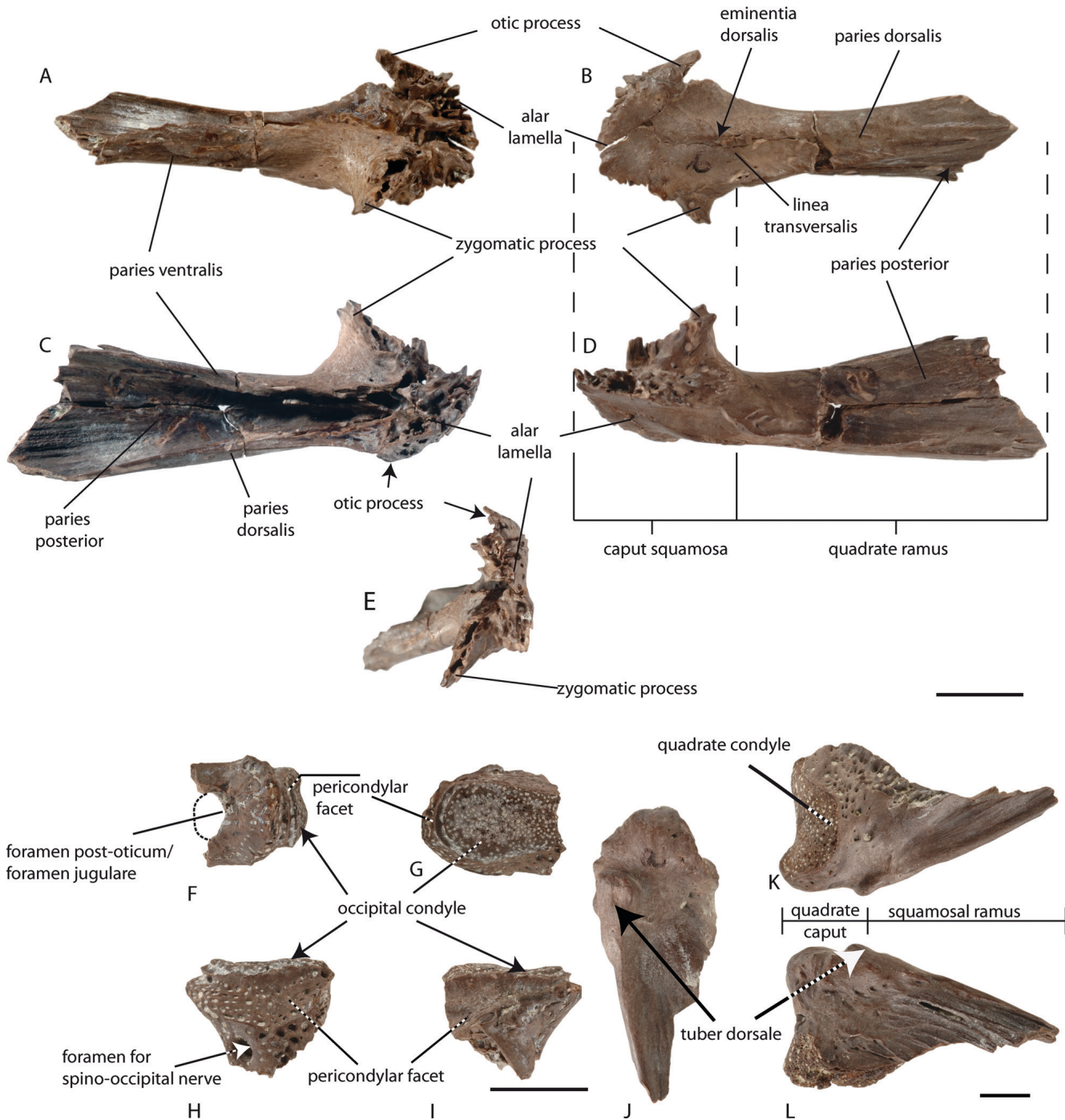


FIGURE 5. Squamosal, occipital, and quadrate of *Ukrainurus hypsognathus*, gen. et sp. nov. Squamosal (NMNHK 22-1711sq-a) in **A**, ventral; **B**, dorsal; **C**, anterior; **D**, posterior; and **E**, medial views; occipital (NMNHK 22-1711oc) in **F**, lateral; **G**, posterior; **H**, ventral; and **I**, dorsal views; quadrate in **J**, anterior; **K**, ventral; and **L**, dorsal views (NMNHK 22-1711q-a). Scale bars equal 1 cm (**A–I**) and 5 mm (**J–L**). (Color figure available online.)

ventromedially into the neural canal. The dorsal surface of the centrum, under the neural arch and directly below the projecting processes, is pierced by small neural canal foramina. These foramina are connected by canals with the foramina that penetrate the dorsal surface of the arterial canal.

A moderately vaulted neural arch is more or less present in all specimens. Its anterior-most part has a smooth surface and connects the left and right prezygapophyses. Posterior to this surface,

the neural arch possesses either no neural spine (on the small vertebrae NMNHK 22-1706-88b, NMNHK 22-1706c) or a poorly developed, low spine with a barbed and wrinkled surface (NMNHK 22-1699, NMNHK 22-1704, NMNHK 22-1705, NMNHK 22-1706). The neural spine arises at the level of the prezygapophyses and extends posteriorly. The posterior portion of the neural arch (pterygapophysis) is broken off in all specimens. There is a single preserved, isolated pterygapophysis that belongs to the

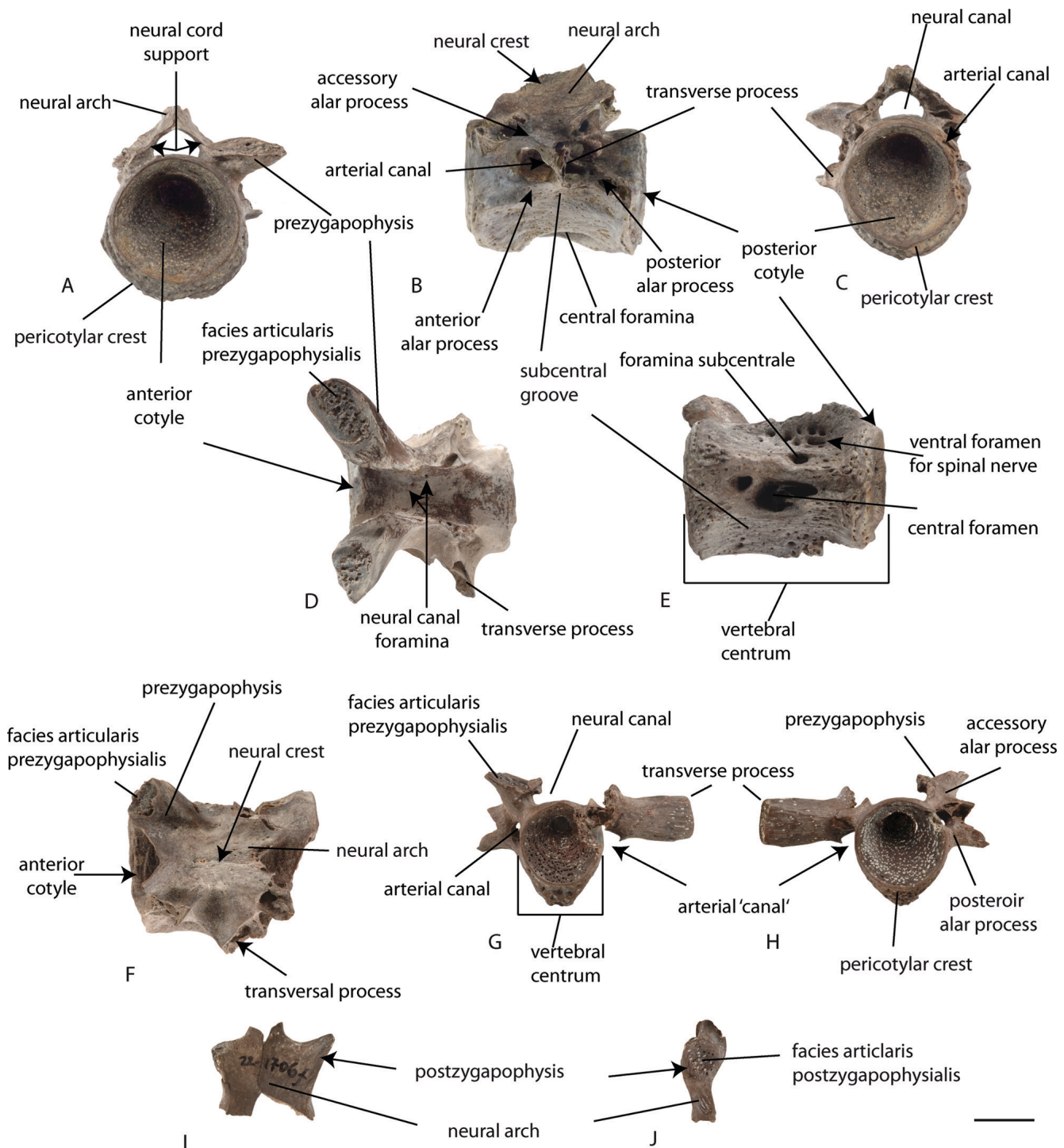


FIGURE 6. Trunk vertebrae of *Ukrainurus hypsognathus*, gen. et sp. nov. **A, G**, anterior (NMNHK 22-1105, NMNHK 22-1706b); **B**, lateral (NMNHK 22-1699); **C, H**, posterior (NMNHK 22-1105, NMNHK 22-1706b); **D, F**, dorsal (NMNHK 22-1698, NMNHK 22-1706), and **E**, ventral (NMNHK 22-1705) views. **I**, anterior and **J**, lateral views of vertebral pterygapophysis (NMNHK 22-1706f). Scale bar equals 1 cm. (Color figure available online.)

smaller individual and that has asymmetric right and left parts. The dorsal surface is smooth and does not possess a neural crest (Fig. 6).

The prezygapophyses are large, strongly elongated, and are anchored between the lateral corners of the neural arch and the centrum. The prezygapophyses possess the facies articularis prezy-

gapophysis on the dorsal side of their anterior portion. This articulation surface has an extremely elongated elliptical form. It is covered with mineralized, strongly porous cartilaginous tissue. The posterior portion of the prezygapophyseal crest joins the lamina (accessory alar process) interconnecting the transverse processes.

The postzygapophyses are preserved only on an isolated pterygapophysis (see above). In this specimen, the postzygapophyses are placed dorsolaterally to the pterygapophysis and project ventromedially. Their articulation facets are irregular circles. The ‘interzygapophyseal ridge,’ extending between pre- and postzygapophyses, is extremely poorly developed or absent.

The transverse processes in all specimens are completely broken off. There is only one vertebra with a preserved right transverse process, but this specimen is pathologically developed because there is no connection between the transverse process and the subcentral ridge (Fig. 6G, H). The proximal end of the transverse process is triangular in cross-section. Between the medial surfaces of the transverse process and the vertebral centrum the arterial canal for the arteria vertebralis is enlarged (Francis, 1934). It is apparent in anterior view that the transverse processes are directed slightly posteroventrally.

Caudal Vertebra—Only a single caudal vertebra (NMNHK 22-1706e; Fig. 6A–E) is preserved. The hemal processes are broken off. The centrum has a similar structure to that seen in the trunk vertebrae. The neural arch, pre- and postzygapophyses, as well as the transverse processes are broken off. The transverse process seems to have extended posteroventrally, as in Recent species. The proximal end of the transverse process is smaller than those of the trunk vertebrae. The foramina of the arterial canal and the ventral foramina for the spinal nerve are of the same size and are situated near each other. The anteroposterior groove of the vertebral centrum, which passes through the central foramina, is considerably deeper than that of the trunk vertebrae and reaches the middle of the vertebral centrum. The ventral surfaces of the posterior cotyle possess posterodorsally projecting hemal processes that are located posterior to the anteroposterior groove. The bases of the hemal processes have an oval form (Fig. 7E).

Ribs—Six right and left ribs are available from different trunk vertebrae (Fig. 7F–I). The rib morphology is the same as in Recent cryptobranchids, *An. scheuchzeri*, and *Z. beliaejae* (locality Korsak B, IP ZSN-K-14). In particular, the ribs are bent at midlength and the bone surface is generally smooth. However, numerous foramina and small protuberances are visible on the anterior and posterior sides (Fig. 7F, G), which are lacking in other giant salamanders.

In the proximal part, the ribs are anteroposteriorly flattened and the anterior and posterior surfaces are concave. The rib articulation surface with its transverse process is unicapitate and has a dumbbell shape. The upper articulation surface is elongated elliptically, whereas the lower one is oval. Both surfaces are connected by a slender strip (Fig. 7H, I). The distal part of the ribs is slender and slightly dorsoventrally depressed and therefore forms an anteroposteriorly elongated elliptical shape in cross-section.

Long Bones

Femur—The femur is a relatively long (67.3 mm) bone with a broken distal end. In lateral view, the bone is dumbbell-shaped. The femur has a lateromedially compressed distal end and an anteroposteriorly compressed proximal end. The distal end is larger than the proximal end. The femur is cylindrical in the middle part (Fig. 8). The bone compactness value at mid-diaphyseal position (Fig. 8C') is 0.87 (Table 2).

The distal end of the femur is enlarged to form a rounded, spoon-shaped head. The head is slightly convex on its lateral surface and concave on its medial surface (trochlear groove) (Fig. 8B, B'). In ventral view, the distal end is triangular. The mineralized cartilaginous tissues that cover the distal articulation surfaces are visible. The femur narrows about 2.5 times distally towards the midshaft and becomes cylindrical. Towards the distal end, the femur doubles in width lateromedially. The proximal end is rectangular, has rounded corners, and forms

TABLE 2. Bone density values of studied giant salamanders femora at the mid-diaphyseal position.

Taxon	n	Value	Reference
<i>Ukrainurus hypsognathus</i> (NMNHK 22-1707)	1	0.87	This study
<i>Andrias japonicus</i>	1	0.979	Laurin et al. (2004)
<i>Cryptobranchus alleganiensis</i>	1	0.966	
<i>Onychodactylus fischeri</i>	1	0.926	

the acetabulofemoral joint. It has an anteriorly slightly concave surface and exhibits a foveal depression (Francis, 1934). The medial surface of the femur possesses a femoral (trochanteric) crest (linea aspera sensu Osawa, 1902). It begins at the middle part of the diaphysis and extends to the anteroventral corner of the proximal end near the highly damaged trochanter. The posterior surface of the bone is wrinkled.

Terminal Phalanges—Two relatively large terminal phalanges are available. The phalanges are slender, relatively long, and have a broad proximal base (3.3 mm) (Fig. 8). They are characterized by a mineralized cartilaginous proximal epiphysis (Fig. 8B). From the base, the terminal phalange becomes less broad toward the rounded tip. The tip possesses a rounded, robust bulb ventrally (Fig. 8B). The base of the phalange from the ventral side is pierced by a laterally stretched ‘foramen.’ The lateral surface of the phalange bears a lateral ridge, stretching from the basis of bulb to the middle part of phalange.

DISCUSSION

Taxonomic Status of *Ukrainurus hypsognathus*

Ukrainurus hypsognathus, gen. et sp. nov., shares with all crown cryptobranchids several characteristics, such as large body size (0.5–2 m); massive bones; dentaries joined along the ventrocaudal portion of the symphysis; parietal and squamosal in direct contact; trochanter fused with the proximal head of the femur; and trunk ribs and distal end of transverse processes of trunk vertebrae unicapitate. The new taxon differs from *Andrias scheuchzeri*, *An. davidianus*, *Zaissanurus beliaejae*, and *Aviturus exscratus* by having less bone ossification; i.e., the compact bone is very thin, the cancellous bone is highly porous, and the medullary cavity is extremely extended (Fig. 3; Tables 1, 2). Moreover, *U. hypsognathus* has two pronounced medullary cavities in the anterior region with relatively large ‘satellite’ cavities. Crown cryptobranchids do not have differentiated medullary cavities, but rather many small- to middle-sized satellite cavities (Fig. 3B).

Ukrainurus hypsognathus, gen. et sp. nov., possesses a number of autapomorphies: (1) the dentary is high and lateromedially compressed; (2) the ventral keel of the dentary is long due to a lateromedial compression of the bone; (3) the pars dentalis is lower than the corpus dentalis in cross-section of the anterior part of the dentary, instead of equal or subequal (Fig. 3); (4) the pars dentalis of the dentary not only produces a dental lamina, bearing the tooth pedicels, but also a smooth subdental lamina; (5) the subdental shelf is plain to very shallow, instead of deep; (6) the longitudinal flange of the labial side of dentary is prominent and has a rugose to pustular and pointed surface, instead of a poorly developed longitudinal flange that is smooth or slightly wrinkled; (7) large mental foramina; (8) lingual crista present on the lingual surface of the dentary; (9) coronoid facet of the articular broad and with highly prominent pit-and-ridge sculpture; (10) nearly invisible, articular-dentary articulation facet at the posterior part of the articular; (11) the prezygapophyses and the facies articularis prezygapophysis extremely elongated and elliptical, instead of round or moderately elongated; (12) eminentia

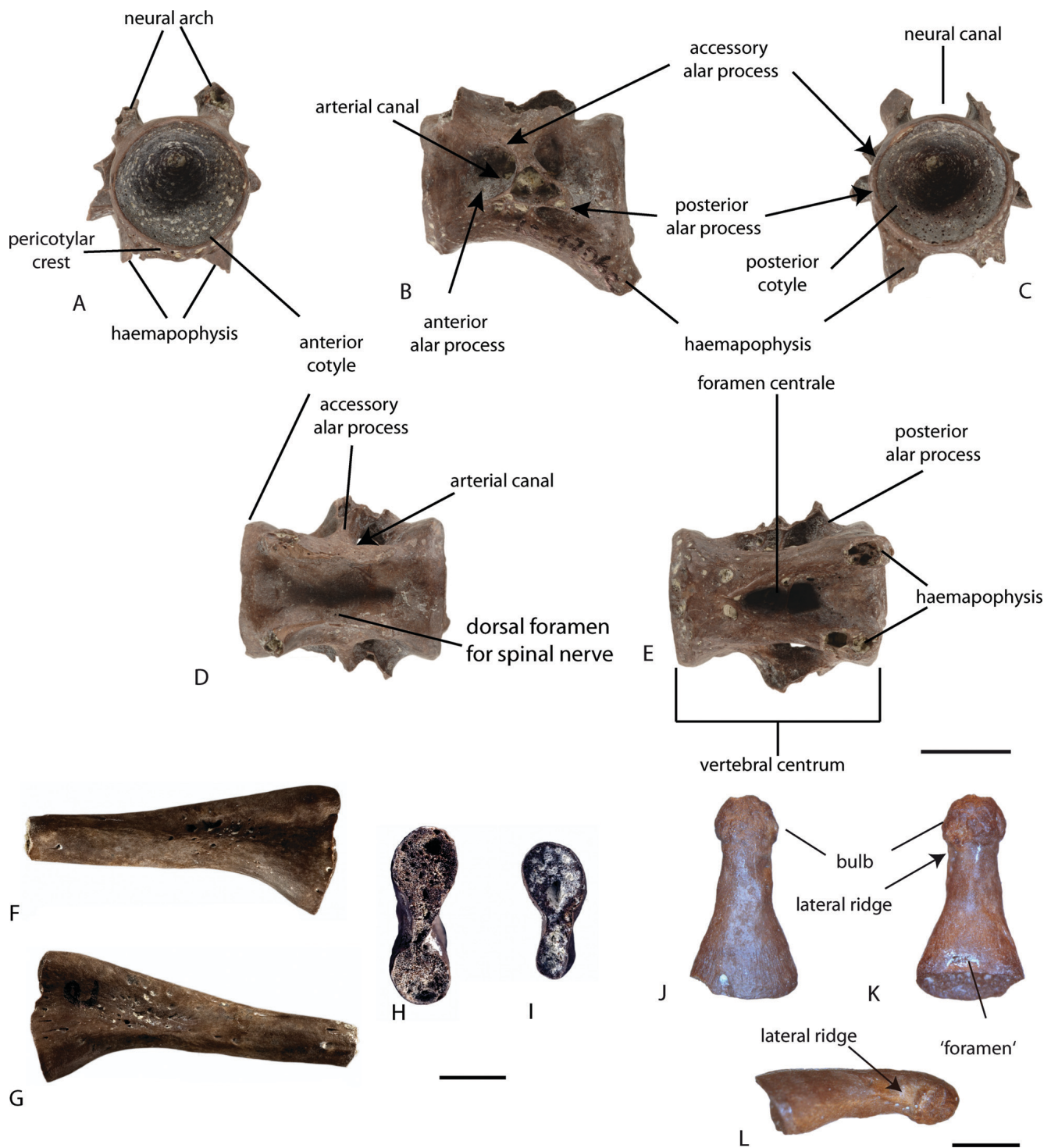


FIGURE 7. Caudal vertebra (NMNHK 22-1706e), ribs, and phalanges of *Ukrainurus hypsognathus*, gen. et sp. nov. Caudal vertebra in **A**, anterior; **B**, lateral; **C**, posterior; **D**, dorsal, and **E**, ventral views; ribs in **F**, anterior and **G**, posterior views (NMNHK 22-1707a.e); rib articulation surface with transverse process of vertebrae (**H**, NMNHK 22-1707a.e and **I**, NMNHK 22-1707a.a); and terminal phalanges (NMNHK 22-1711f.1) in **J**, dorsal; **K**, ventral, and **L**, lateral views. Scale bars equal 1 cm (**A–E**), 5 mm (**F–I**), and 2 mm (**J–L**). (Color figure available online.)

dorsalis present on squamosal; (13) pericondylar facet of occipital broad, instead of slightly pronounced or absent; (14) posterior paries of squamosal high and forming obtuse angle with paries dorsalis, instead of low and parallel to paries dorsalis; (15) paries posterior of squamosal large and zygomatic process directly an-

terolaterally, instead of anteromedially; (16) dorsal margin of caput squamosal lack marginal lamina; and (17) low bone density values for the dentary (Table 1) and femur (Table 2).

Ukrainurus hypsognathus, gen. et sp. nov., shares a number of homoplastic or symplesiomorphic features with various

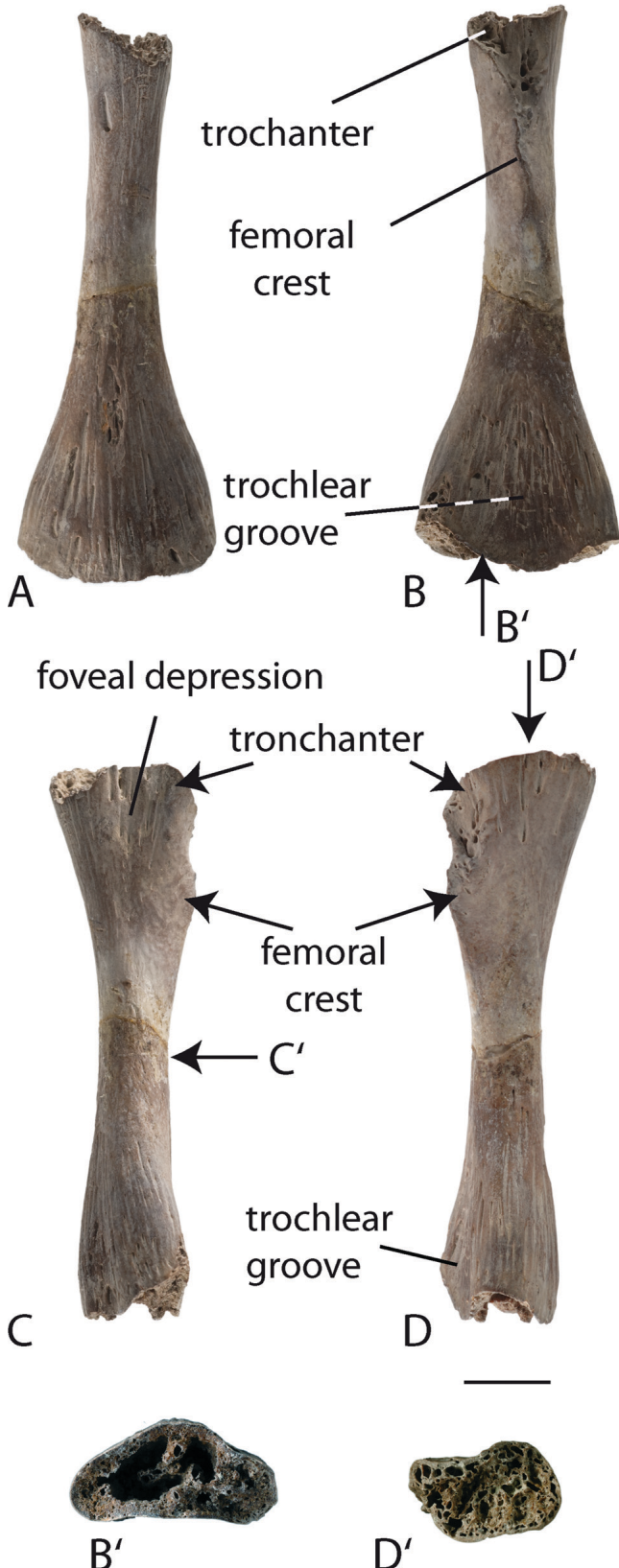


FIGURE 8. Right femur of *Ukrainurus hypsognathus*, gen. et sp. nov. (NMNHK 22-1707) in **A**, dorsal; **B**, ventral; **C**, posterior; and **D**, anterior views; **B'**, distal and **D'**, proximal articulation surface of femur; **C'**, the arrow shows the mid-diaphyseal position of the bone. Scale bar equals 1 cm. (Color figure available online.)

fossil and living pancryptobranchans. The mandibular symphysis is elliptically elongated as in '*Cryptobranchus*' *saskatchewanensis* (Naylor, 1981:fig. 1A), instead of round to slightly elliptical as all other giant salamanders. The ventral symphyseal cartilage is small, as in 'C.' *saskatchewanensis*, whereas *Andrias* spp. and *Cryptobranchus* *alleganiensis* have a (~1.5 times) larger cartilage. *Ukrainurus hypsognathus* resembles *Av. exsecratus* in having highly pronounced perichondral ossification on the dentary, the femoral trochanter crest, and neural crest, and by having pierced bone surfaces in the femur, ribs, and vertebrae. The new species and *An. scheuchzeri* have a smooth lingual surface of the corpus dentalis, although an 'S'-shaped concavity is nevertheless apparent in *An. scheuchzeri*. In comparison, *Av. exsecratus* (Gubin, 1991:fig. 6, table 8), *Z. beliajevae* (Chkhikvadze, 1982:figs. 1, 2, pl. 1), and 'C.' *saskatchewanensis* (Naylor, 1981:fig. 1) have a deep groove (presymphyseal sulcus) on the lingual surface of the corpus dentalis between the symphysis and the anterior limit of the Meckelian cartilage, under the lamina dentalis, and *An. davidianus*, *An. japonicus*, and *C. alleganiensis* have a concave surface in this region.

U. hypsognathus differs from Recent giant salamanders in having a long and broad coronoid process, whereas in the Recent species and *Z. beliajevae* (IP ZSN-K-11) it is long and narrow, and in *An. scheuchzeri* short and broad (for size relation see Appendix 1).

The femur of the fossil species is similar to those of *C. alleganiensis* (ZFMK 5245), *Andrias* spp. (e.g., ZFMK 76996), and *Z. beliajevae* (Chkhikvadze, 1982:fig. 8, pl. 3), but differs from *Av. exsecratus* (Gubin, 1991:fig. 4, table 9), which has the longest femur crista, ending at the left ridge of the trochlear groove. However, *U. hypsognathus* shows the lowest value of femoral bone density at the mid-diaphyseal position (Fig. 8; Table 2).

Two terminal phalanges were found in the fossil remains, which belong to a large amphibian. There are only two large size amphibians from the Grytsiv locality: *Latonia gigantea* (Lartet, 1851) and *Ukrainurus hypsognathus*, gen. et sp. nov. However, the fossil phalanges could be distinguished from *Latonia gigantea* (Discoglossidae) and grouped with Pancryptobrancha by having (1) a lateral ridge between the basis of the bulb and the middle part of phalange (Fig. 7K; this feature is lacking in discoglossids; Kamermans and Vences, 2009); and (2) the phalanges have the same mineralized cartilage tissue at their base as the other long bones of *U. hypsognathus*, gen. et sp. nov. However, despite these similarities, the terminal phalanges differ from those of *An. davidianus*, *An. japonicus*, *An. scheuchzeri*, and *C. alleganiensis* in having a different terminal morphology. The phalanges of the new fossil species are slender, relatively long, and end with a rounded bulb on the ventral surface, whereas in *An. japonicus*, *An. davidianus*, and *An. scheuchzeri* the phalanges are robust, without an expressed bulb on the ventral tip, and in *An. davidianus* and *C. alleganiensis* the lateral ridges can extend to the tip and form a claw-like structure. In *An. japonicus*, *An. scheuchzeri*, *C. alleganiensis*, and *U. hypsognathus*, the lateral ridges are less pronounced than in *An. davidianus*.

The new species can be distinguished from all known pancryptobranchans by the extremely elongated, elliptical prezygapophyses and prezygapophyseal articulation surfaces. Other giant salamander species have short or slightly prolonged, round or elliptical prezygapophyses and prezygapophyseal articulation surfaces, but none of them reach this form. *Ukrainurus hypsognathus* has no interzygapophyseal ridge, a feature common in all other pancryptobranchans with the exception of *Av. exsecratus*, which has a well-developed interzygapophyseal ridge (Gubin, 1991:figs. 2, 3, pl. 9).

The transverse processes of all vertebrae in the new fossil species seem to be directed slightly posteroventrally, as in several trunk vertebrae of *Av. exsecratus* (Gubin, 1991:fig. 2, pl. 9). However, data from the literature (*An. japonicus*, Shikama and

Hesegawa, 1962:figs. 6–9, pl. 29; *Av. exsecratus*, Gubin, 1991; *Andrias* sp., Matsui et al., 2001:fig. 1A–G, pl. 1) and our observations on Recent (*An. davidianus*, *An. japonicus*, *C. alleganiensis*) and fossil (*An. scheuchzeri*, *Z. beliajevae*) species show that transverse process orientation is variable along the vertebral column within individuals. Transverse processes on the anterior trunk vertebrae are generally oriented posteriorly or posterodorsally. The posterior trunk and caudal vertebrae, by contrast, have posteroventrally directed transverse processes. However, more well-preserved specimens would be needed to interpret the systematic significance of this character and its distribution within this species.

The pterygapophyses of the new taxon are asymmetric. However, this is a common feature among fossil and Recent pancryptobranchans. Asymmetry can also be found in other skeletal elements, such as the squamosal, articular, and transverse processes. In addition to asymmetry of individual bones, cryptobranchids can also show pathological development in the skeleton, for example, a skeleton of *An. davidianus* with double left or right postzygapophyses (ZFMK 90469), and *Andrias japonicus* with double left transverse processes on the 19th vertebra (one of two ZNHM unnumbered skeletons; Westphal, 1958:5). Among the trunk vertebrae of *U. hypsognathus*, an abnormal development of the transverse process is present (Fig. 7G, H).

The form and position of the hemal process of the caudal vertebrae in *Ukrainurus hypsognathus* differ from those of all fossil and Recent crown cryptobranchids. The base of the hemal process has an elongated oval form, whereas in Recent forms the process invests on lamella-like structures, forming the lateral walls of the hemal canal. In the Grytsiv species, the processes originate from the posterior portion of the vertebral centrum, whereas the Recent giant salamanders, *An. scheuchzeri*, and *Av. exsecratus*, have hemal processes located in the middle part of the centrum. Moreover, the arterial canal of the Grytsiv form is larger and has a broader opening in comparison to these taxa, which have very narrow arterial canals, with small foramina.

Phylogenetic Considerations

We constructed a data matrix that includes all Tertiary and Recent pancryptobranchans to assess the phylogenetic affinities of *Ukrainurus hypsognathus*, gen. et sp. nov. We purposefully restricted ourselves to Cenozoic taxa, because all putatively related Mesozoic forms (e.g., *Eoscaphepeton asiaticum* and *Horezmia gracilis*) are known from fragmentary material or larvae and/or subadults (*Chunerpeton tianyiensis*) only and lack characters that would allow diagnosing them a priori as being situated close to or within crown group Cryptobranchidae, our clade of interest. Furthermore, we exclude *Andrias karalchepaki* Chkhikvadze, 1982, from the Miocene of Kazakhstan, because this taxon is too poorly known. The monophyly of our ingroup is supported by the following list of characters: trunk ribs unicapitate (character 32); body size large (character 33); and parietal and squamosal in contact with one another (character 34). Our sources for all character observations are listed in Materials and Methods. The final character-taxon matrix consists of 39 characters for eight ingroup taxa and one outgroup taxon. Only 13 characters, however, are parsimony informative. The basal hynobiid salamander *Onychodactylus fischeri* (Zhang et al., 2006) served as the outgroup taxon. The matrix was analyzed using PAUP, version 4.0b10 (Swofford, 2002). The character list is provided in Appendix 1 and the character-taxon matrix in Appendix 2 and the online Supplementary Data.

For the first phylogenetic analysis, all taxa were included, all characters were considered of equal weight, the only available multistate character was left unordered, and branches were set to collapse if their minimum length was zero. An exhaustive search retrieved 40 most parsimonious trees (MPTs) with 46 steps.

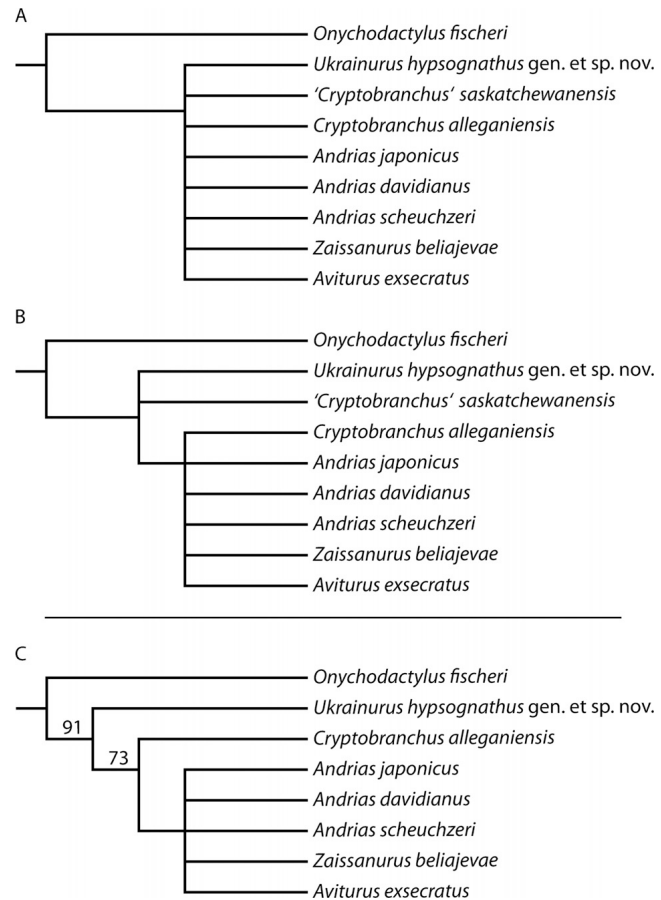


FIGURE 9. Phylogenetic analysis of the interrelationships of cryptobranchids. **A**, strict consensus tree and **B**, Adams consensus tree of the first phylogenetic analysis. **C**, strict consensus, Adams consensus, and 50% majority consensus topology retrieved from the second phylogenetic analysis. Bootstrap support values >50% are shown next to the corresponding node (1000 replicates).

The consistency index is 0.65 when all parsimony uninformative characters are removed. The strict consensus topology (Fig. 9A) reveals a complete lack of resolution because all ingroup taxa are arranged in a polytomy. The basal placement of '*Cryptobranchus*' *saskatchewanensis* within the Adams consensus topology (Fig. 9B), however, indicates that this taxon causes much of this lack of resolution. This is not surprising, given that we were only able to score this taxon for six parsimony informative characters.

For the second analysis, we used the same parameters as in the first analysis, but omitted '*C.*' *saskatchewanensis* and ran a bootstrap analysis with 1000 randomly seeded replicates. The exhaustive search this time retrieved only four MPTs of 43 steps. The strict, Adams consensus and 50% consensus topologies are identical (Fig. 9C). The consistency index is 0.76 after removal of all parsimony uninformative characters. All four topologies agree by placing *U. hypsognathus* as the sister group to crown Cryptobranchidae and by placing the North American *Cryptobranchus alleganiensis* as the sister group to all Eurasian cryptobranchids. Characters that unite crown Cryptobranchidae to the exclusion of *U. hypsognathus* include the presence of a deep dental shelf (character 8), a pronounced articulation facet between the articular and dentary (character 13), a narrow articular condyle (character 16), and the presence of only slightly elongated

articular surfaces of the prezygapophyses (character 25). The monophyly of Eurasian cryptobranchids is supported by the presence of low enamel caps (character 12) and the presence of only three bones around the nares (character 39). It must be noted, however, that both of these characters cannot be observed among the fossil Eurasian cryptobranchids *Aviturus exsecratus* and *Zaissanurus beliajevae*.

The unclear phylogenetic placement of '*C.*' *saskatchewanensis*, and a number of derived similarities between '*C.*' *saskatchewanensis* and *U. hypsognathus* (i.e., presence of a elongated elliptical symphysis [character 1]; presence of a small triangular space between the dentaries [character 2]), and a lack of shared derived characters between '*C.*' *saskatchewanensis* and *C. alleganiensis* further lead us to conclude that '*C.*' *saskatchewanensis* may be a stem cryptobranchid and, therefore, not closely related to *C. alleganiensis*.

The Mesozoic taxa *Chunerpeton tianyiensis*, *Eoscaphelepon asiaticum*, and *Horezmia gracilis* have previously been referred to Cryptobranchidae (Gao and Shubin, 2003; Skutschas, 2009). Our phylogenetic analysis allows us to speculate about their placement with respect to Pancryptobranchia. None of these taxa can be scored for the list of characters that unite crown Cryptobranchidae or the clade of Asian cryptobranchids (see above). We therefore do not have any positive or negative evidence that would allow us to exclude them from or include them in these clades. However, it is apparent that characters that unite the relatively derived *U. hypsognathus* clade are absent from these taxa. In particular, *Ch. tianyiensis* lacks a parietal/squamosal contact, *E. asiaticum* lacks a trochanter that is fused with the proximal head of the femur, and *H. gracilis* lacks large body size. All three taxa are therefore most parsimoniously placed outside of the *U. hypsognathus* clade positioned along the cryptobranchid stem lineage and should not be used to calibrate the age of the cryptobranchid crown group. We encourage others to more rigorously test the phylogenetic position of *Ch. tianyiensis*, *E. asiaticum*, and *H. gracilis* using more inclusive character matrices and hope that our analysis will serve as a good starting point.

Our phylogenetic results imply a taxonomy that is substantially different from that of Gubin (1991), who subdivided Cryptobranchidae into the subclades Aviturinae (*Zaissanurus beliajevae*, *Ulanurus fractus*, *Aviturus exsecratus*, and probably '*Cryptobranchus*' *saskatchewanensis* and *Cryptobranchus matthewi*) and Cryptobranchinae (*Cryptobranchus alleganiensis* and *Andrias* spp.). The characters that Gubin (1991) used to support his taxonomy are listed in Table 3.

Many of the characters provided by Gubin (1991) need critical consideration. No size estimates are available for *U. fractus*, '*C.*' *saskatchewanensis*?, and *C. matthewi*?, whereas the largest specimen of genus *Andrias* (both fossil and Recent species) can reach

body lengths of more than 170 cm (Estes, 1981; Murphy et al., 2000; Matsui et al., 2008). We therefore cannot support the supposed distribution of this character (see in Table 3) and cannot discover an alternative pattern either.

Long hind limbs are indeed present in *Aviturus exsecratus*, but this character cannot be observed among all other representatives of Aviturinae. Similarly, *Av. exsecratus* is the only giant salamander known to have a long parietosquamosal suture. Until more evidence is available, we therefore consider both of these characters to be autapomorphic for *Av. exsecratus* and not to be diagnostic of a more inclusive clade.

Gubin (1991) furthermore distinguished his two subfamilies of giant salamanders based on the number of teeth in the dentary tooth row. However, the number of teeth is known to be highly variable even within species and also shows no relationship to size or age of the individual (Böttcher, 1987; pers. observ. of *Andrias davidianus*, *An. japonicus*, *An. scheuchzeri* by D.V.). Until full variation has been documented for each species, it is not possible to draw any phylogenetic conclusions from this character. The same argument can be made for vertebral shapes. Gubin (1991) argued that *Cryptobranchus alleganiensis* and *Andrias* spp. only have rectangular vertebrae, but our observations of the relevant material demonstrate that every individual appears to have a different vertebral shape (also see Böttcher, 1987). It therefore appears that none of the characters listed by Gubin (1991) contradict the phylogenetic analysis that we present herein (Fig. 9).

The Taxonomic Validity of *Ulanurus fractus*

The type locality of *Aviturus exsecratus* has yielded another species of cryptobranchid, *Ulanurus fractus*, and our assessment of character-state distribution and variation in cryptobranchids allows us to reevaluate the validity of the latter species. *Ulanurus fractus* was erected based on two fragmentary dentaries (Gubin, 1991:103, PIN 4357/27, PIN 4358/2) and diagnosed by (1) the presence of a presymphysial sulcus; (2) the presence of tooth-like crests within the presymphysial sulcus; and (3) the presence of longitudinal grooves within the presymphysial sulcus. The type material of *Ulanurus fractus* indeed possesses a presymphysial sulcus at the corpus dentalis, but this is also present in the holotype of *Av. exsecratus*. Similarly, although tooth-like crests and longitudinal grooves are present in the type material of *U. fractus*, tooth-like crests and longitudinal grooves are also known from some *Av. exsecratus* specimens (PIN 4357/32 and IP ZSN-KKS-1, respectively). It is therefore apparent that *U. fractus* was diagnosed based on characters that are present in the coeval *Av. exsecratus* and we therefore consider *Ulanurus fractus* to be a junior synonym of *Aviturus exsecratus*.

TABLE 3. Characteristic features of the giant salamander subfamilies Aviturinae and Cryptobranchinae according to Gubin (1991).

	Aviturinae Gubin, 1991	Cryptobranchinae Cope, 1889
Taxa included	<i>Zaissanurus beliajevae</i> , <i>Ulanurus fractus</i> , <i>Aviturus exsecratus</i> , ' <i>Cryptobranchus</i> ' <i>saskatchewanensis</i> , <i>Cryptobranchus matthewi</i>	<i>Cryptobranchus alleganiensis</i> , <i>Andrias</i> spp.
Features		
1	Very large animals, body length at least 150–170 cm, hind extremities up to 25 cm long	Animals with relatively short extremities (length of femur less than twice the length of centra of trunk vertebrae)
2	Length of parietal-squamosal suture less than two-thirds of parietal length? along the axial line; tubercle absent along the suture line	Suture between parietal and squamosal bones short; bones form a tubercle at point of contact
3	Tooth row of dentary has >100 teeth and is separated from the 'sulcus dentalis' (subdental shelf) by a wide smooth area (subdental lamina?)	Tooth row of dentary has 60–75 teeth; tooth bases lie directly above 'sulcus dentalis' (subdental shelf sensu this study)
4	Vertebrae rectangular, trapezoid, or parallelogram-shaped in profile	Vertebrae always rectangular in lateral view
5	Prezygapophyses do not project above the base of bony processes	Prezygapophyses usually project above bases of bony processes

Biogeographic and Temporal Considerations

The outgroup taxon and the majority of our ingroup taxa originate from Eurasia, with the exception of *Cryptobranchus alleganiensis* and ‘C.’ *saskatchewanensis*. If geography is treated as a character and mapped onto the phylogenetic tree, it becomes apparent that the common ancestor of our ingroup lived in Asia and that the ancestor of *C. alleganiensis* and ‘C.’ *saskatchewanensis* migrated to North America independently from one another (DELTRAN). The alternative (ACCTRAN) interpretation that the cryptobranchid lineage dispersed to North America, only to later return to Eurasia, appears less likely, because the panhypobranchian record is rather continuous in Eurasia. The oldest representative of crown Cryptobranchidae is *Aviturus exsecratus* from the terminal Paleocene of the Nemegt Basin, Mongolia. This finding predicts that the basal split of crown Cryptobranchidae must have occurred prior to the terminal Paleocene, possibly even as early as the Late Cretaceous, but it remains unclear when the *C. alleganiensis* lineage dispersed into North America.

Diet and Food Consumption

Mandible Movement—During prey capture and prey manipulation, the mandibles of *Cryptobranchus alleganiensis* and *Andrias* spp. sometimes flex around the mandibular symphysis. This movement is permitted by two pads of elastic cartilage that are situated between the dentaries and that are lacking in many other groups of salamanders. This asymmetric movement is largely related to the size of the larger ventral pad, which fills a large, triangular, ventral space between the dentaries (Cundall et al., 1987). *Ukranurus hypsognathus* has a smaller space for the elastic cartilage relative to all crown cryptobranchids. We therefore assume that it possessed a less flexible mandibular joint and was therefore not able to feed as asymmetrically as Recent cryptobranchids.

Musculature—Using the observations of Buckley et al. (2010), that in plethodontine salamanders the degree of robustness of the squamosal is related to the overall strength of the jaws and the sizes of the mandibular levator muscles and associated otic and squamosal crests, we can make some conclusions about musculature and bite force in fossil giant salamanders. *Ukranurus hypsognathus* has the most robust squamosal among all known Recent and fossil panhypobranchians. The coronoid process is particularly long and broad. On the dorsal side, the process partially or completely serves as the site of origin for four groups of mandibular levator muscles (deep mandibular levator, levator mandibulae posterior, levator mandibulae externus, and superficial levator mandibulae anterior; Elwood and Cundall, 1994). Taking into account the size proportions of the process in the Recent species, *Zaissanurus beliaevasi*, and *Andrias scheuchzeri*, we conclude that larger and stronger mandibular levator muscles must have been present in the new species. The bone surfaces where the tendons of the large levator mandibulae externus (paries dorsalis of squamosal), small levator mandibulae posterior (anterolateral surface of squamosal), and anterior depressor mandibulae (medial tip and paries posterior of squamosal) attach are also larger than in Recent species. Finally, the pericondylar surfaces of the occipital are greatly enlarged. All of these observations allow us to conclude that the new taxon had a particularly strong biting force and was able to seize large prey with relative ease.

A diverse assortment of vertebrate prey taxa were available for *Ulanurus hypsognathus*. These include adults and larvae of the amphibians *Microteles caucasicus*, *Chelotriton paradoxus*, Salamandridae sp., *Palaeobatrachus* sp., *Pelobates* cf. *decheni*, *Pelobates* sp., *Bufo* sp., *Latonia gigantea* (Zerova, 1985; Korotkevich, 1988; Rage and Roček, 2003; Roček, 2005), and *Pelophylax (ridibundus)* sp. (pers. observ.), as well as the fishes *Esox* sp., Siluridae indet., and Cyprinidae indet. (pers. observ.). There is no invertebrate fossil record from the Grytsiv locality.

ACKNOWLEDGMENTS

We thank J. Prieto, M. Aiglstorfer, and P. Havlik (Institute for Geosciences, University of Tübingen) for providing comparative material of *Andrias scheuchzeri* (J.P.) and their valuable comments on an earlier version of the manuscript. The photographs in Figures 2–12 were produced by W. Gerber (University of Tübingen). We are indebted to E. Schwaderer (Department of Radiology, University of Tübingen) for computer tomography of fossil and Recent cryptobranchid bones. We are grateful to J. Anderson for editorial comments and to J. Gardner and J.-C. Rage for criticism and constructive reviews. This project was supported by the Deutsche Forschungsgemeinschaft (DFG), grant BO 1550/14 (to M.B.).

LITERATURE CITED

- Averianov, A., and L. Tjutkova. 1995. *Ranodon* cf. *sibiricus* (Amphibia, Caudata) from the upper Pliocene of southern Kazakhstan: the first fossil record of the family Hynobiidae. *Paläontologische Zeitschrift* 69:257–264.
- Blanchard, É. 1871. Note sur une nouvelle salamandre gigantesque (*Sieboldia davidi* Blanch.) de la Chine occidentale. *Comptes Rendus hebdomadaires des Séances de l'Académie des Sciences* 73:79–80.
- Böhme, M., and A. Ilg. 2003. fosFARbase. Available at www.wahre-staerke.com. Accessed December 1, 2011.
- Böttcher, R. 1987. Neue Funde von *Andrias scheuchzeri* (Cryptobranchidae, Amphibia) aus der süddeutschen Molasse (Miozän). *Stuttgarter Beiträge für Naturkunde, Serie B* 131:1–38.
- Boulanger, G. A. 1886. First report on additions to the batrachian collection in the Natural-History Museum. *Proceedings of the Zoological Society of London* 1886:411–416.
- Buckley, D., M. H. Wake, and D. B. Wake. 2010. Comparative skull osteology of *Karsenia koreana* (Amphibia, Caudata, Plethodontidae). *Journal of Morphology* 271:533–558.
- Chepalyga, A. L., V. M. Korotkevich, Trubikhin, V. M., and T. V. Svetliskaya. 1985. Chronology of the eastern Paratethyan regional stages and *Hippurion* faunas according to palaeomagnetic data; pp. 137–139 in F. Rögl (ed.), 7th Congress of the Regional Committee on Mediterranean Neogene Stratigraphy (RCMN): Abstract Book of Symposium on European Late Cenozoic Mineral Resources. Hungarian Geological Society, 15–22 September 1985, Budapest.
- Chernov, S. A. 1959. Fauna of Tadzhikian SSR, Reptiles. Publishing house of Tadzhikian Academy of Sciences, Stalinabad, 204 pp. [Russian]
- Chkhikvadze, V. M. 1982. On the findings of fossil Cryptobranchidae in the USSR and Mongolia. *Vertebrata Hungarica* 21:63–67.
- Cope, E. D. 1889. The Batrachia of North America. *Bulletin of the United States National Museum* 34:1–525.
- Cundall, D. J., J. Lorenz-Elwood, and J. D. Groves. 1987. Asymmetric suction feeding in primitive salamanders. *Experientia* 43:1229–1231.
- Daudin, F. M. 1803. *Histoire Naturelle, Générale et Particulière des Reptiles: Ouvrage Faisant suite à l'Histoire Naturelle Générale et Particulière, Composée par Leclerc de Buffon, et Rédigée par C. S. Sonnini, Membre de Plusieurs Sociétés Savantes*. Dufart, Paris, 439 pp.
- Delfino, M., S. Doglio, Z. Roček, D. Seglie, and L. Kabiri. 2009. Osteological peculiarities of *Bufo bronneri* (Anura, Bufonidae) and their possible relation to life in an arid environment. *Zoological Studies* 48:108–119.
- Didkovsky, V. Y. 1964. Biostratigraphy of Neogene deposits on the southern Russian Platform on the basis of the foraminiferal fauna. Ph.D. dissertation, Institute of Geological Sciences, Academy of Sciences of Ukrainian SSR, Kiev, 40 pp. [Russian]
- Duellman, W. E., and L. Trueb. 1994. *Biology of the Amphibia*. The Johns Hopkins University Press, Baltimore and London, 670 pp.
- Elwood, J. R. L., and D. Cundall. 1994. Morphology and behavior of the feeding apparatus in *Cryptobranchus alleganiensis* (Amphibia: Caudata). *Journal of Morphology* 220:47–70.
- Estes, R. 1981. Gymnophiona, Caudata; in P. Wellnhofer (ed.), *Handbuch der Paläoherpetologie—Encyclopedia of Paleoherpetology*, Volume 2. Gustav Fischer, Stuttgart and New York, 115 pp.
- Francis, E. T. 1934. *The Anatomy of the Salamander*. Clarendon Press, Oxford, U.K., 381 pp.

- Gao, K. Q., and N. H. Shubin. 2003. Earliest known crown-group salamanders. *Nature* 422:424–428.
- Gardner, J. D. 2003. The fossil salamander *Proamphiuma cretacea* Estes (Caudata; Amphiumidae) and relationships within the Amphiumidae. *Journal of Vertebrate Paleontology* 23:769–782.
- Gardner, J. D., and A. O. Averianov. 1998. Albanerpetontid amphibians from the Upper Cretaceous of Middle Asia. *Acta Paleontologica Polonica* 43:453–467.
- Girondot, M., and M. Laurin. 2003. Bone Profiler: a tool to quantify, model, and statistically compare bone-section compactness profiles. *Journal of Vertebrate Paleontology* 23:458–461.
- Greven, H., and G. Clemen. 1980. Morphological studies on the mouth cavity of urodeles. *Amphibia-Reptilia* 1:49–59.
- Greven, H., and G. Clemen. 2009. Early tooth transformation in the paedomorphic Hellbender *Cryptobranchus alleganiensis* (Daudin, 1803) (Amphibia: Urodela). *Vertebrate Zoology* 59:71–79.
- Gubin, Y. M. 1991. Paleocene salamanders from Southern Mongolia. *Palaeontologicheskiy Zhurnal* 33:96–106. [Russian]
- Haeckel, E. 1866. Generelle Morphologie der Organismen. Georg Reimer, Berlin, 574 pp.
- Harzhauser, M., and W. Piller. 2004. Integrated stratigraphy of the Sarmatian (upper Middle Miocene) in the western central Paratethys. *Stratigraphy* 1:65–86.
- Holl, F. 1831. Handbuch der Petrefaktenkunde. P.G. Hilscher'sche Buchhandlung, Dresden, 489 pp.
- Holman, A. J. 2006. Fossil Salamanders of North America. Indiana University Press, Bloomington and Indianapolis, Indiana, 232 pp.
- Hyrtl, J. 1885. *Cryptobranchus japonicus*: schediagma anatomicum, quod almae et antequissimae Universitati Vidonbonensi, ad solennia saecularia quinta, pie celdebranda. Vindobona, G. Braumüller, Vindobona, 132 pp.
- Joyce, W. G., J. F. Parham, and J. A. Gauthier. 2004. Developing a protocol for the conversion of rank-based taxon names to phylogenetically defined clade names, as exemplified by turtles. *Journal of Paleontology* 78:989–1013.
- Kamermans, M., and M. Vences. 2009. Terminal phalanges in ranoid frogs, morphological diversity and evolutionary correlation with climbing habits. *Alytes* 26:117–152.
- Kojumdgieva, E. I., N. P. Paramonova, L. S. Belokrys, and L. V. Muskhelishvili. 1989. Ecostratigraphic subdivision of the Sarmatian after molluscs. *Geologica Carpathica* 40:81–84.
- Korotkevich, E. L. 1988. History of Eastern European *Hipparium* Fauna Formation. Naukova dumka, Kiev, 164 pp. [Russian]
- Korotkevich, E. L., V. N. Kushniruk, Y. A. Semenov, and A. L. Chepaliga. 1985. A new middle Sarmatian vertebrate fauna locality in Ukraine. *Vestnik Zoologii* 29:81–82. [Russian]
- Krakhmalnaya, T. 1996. Hipparians of the Northern Black Sea coast area (Ukraine and Moldova): species composition and stratigraphic distribution. *Acta Zoologica Cracoviensia* 39:261–267.
- Kuzmin, S. L., and B. Thiesmeier. 2001. Mountain salamanders of the genus *Ranodon*. Advances in Amphibian Research in the Former Soviet Union 6:1–200.
- Laurin, M., M. Girondot, and M.-M. Loth. 2004. The evolution of long bone microstructure and lifestyle in lissamphibians. *Paleobiology* 30:589–613.
- Linnaeus, C. 1758. *Systema Naturae*. L. Salvi, Stockholm, 823 pp.
- Lourens, L. J., F. J. Hilgen, J. Laskar, N. J. Shackleton, and D. Wilson. 2004. The Neogene Period; pp. 409–440 in F. M. Gradstein, J. G. Ogg, and A. G. Smith (eds.), *A Geologic Time Scale 2004*. Cambridge University Press, Cambridge, U.K.
- Lungu, A. N. 1978. Hipparium Fauna of Middle Sarmatian of Moldova: Carnivores. Shtints, Kishinev, 140 pp. [Russian]
- Lungu, A. N. 1981. Hipparium Fauna of Middle Sarmatian of Moldova: Insectivores, Lagomorphs and Rodents. Shtints, Kishinev, 135 pp. [Russian]
- Matsui, M., E. Kitabayashi, K. Takahashi, and S. Sato. 2001. A fossil giant salamander of the genus *Andrias* from Kyushu, Southern Japan. *Research Reports Lake Biwa Museum* 18:72–28.
- Matsui, M., A. Tominaga, W.-Z. Liu, and T. Tanaka-Ueno. 2008. Reduced genetic variation in the Japanese giant salamander, *Andrias japonicus* (Amphibia: Caudata). *Molecular Phylogenetics and Evolution* 49:318–326.
- Meszoely, C. 1966. North American fossil cryptobranchid salamanders. *American Midland Naturalist* 75:495–515.
- Murphy, R. W., J. Fu, D. E. Upton, T. De Lema, and E.-M. Zhao. 2000. Genetic variability among endangered Chinese giant salamanders, *Andrias davidianus*. *Molecular Ecology* 9:1539–1547.
- Naylor, B. G. 1981. Cryptobranchid salamanders from the Paleocene and Miocene of Saskatchewan. *Copeia* 1:76–86.
- Nesin, V. A., and A. Nadachowski. 2001. Late Miocene and Pliocene small mammal faunas (Insectivora, Lagomorpha, Rodentia) of southeastern Europe. *Acta Zoologica Cracoviensia* 44:107–135.
- Nessov, L. A. 1981. Cretaceous salamanders and frogs of Kyzylkum Desert. *Proceedings of the Zoological Institute of Academy of Sciences of the USSR* 101:57–88.
- Okajima, K. 1908. Die Osteologie des *Onychodactylus japonicus*. *Zeitschrift für wissenschaftliche Zoologie* A 91:351–381.
- Osawa, G. 1902. Beiträge zur Anatomie des japanischen Riesensalamanders. *Mitteilungen aus der medicinischen Facultät der Kaiserl.-Japan, Universität zu Tokio* 5:1–207.
- Pevzner, M. A., and E. A. Vangengeim. 1993. Magnetochronological age assignments of middle and late Sarmatian Mammalian localities of the Eastern Paratethys. *Newsletters on Stratigraphy* 29:63–75.
- Rage, J. C., and Z. Roček. 2003. Evolution of anuran assemblages in the Tertiary and Quaternary of Europe, in the context of palaeoclimate and palaeogeography. *Amphibia-Reptilia* 24:133–167.
- Reese, A. M. 1906. Anatomy of *Cryptobranchus allegheniensis*. *The American Naturalist* 40:287–326.
- Roček, Z. 2005. Late Miocene Amphibia from Rudabánya. *Palaeontographia Italica* 90:11–29.
- Rögl, F. 1998. Paratethys Oligocene-Miocene stratigraphic correlation. *Abhandlungen der Senckenbergischen Naturforschenden Gesellschaft* 549:3–7.
- Roshka, V. K. 1967. Stratigraphic scheme of Sarmatian sediments in Moldova. *Proceedings of Academy of Sciences Moldavian SSR* 4:72–80. [Russian]
- Scopoli, G. A. 1777. *Introductio ad Historiam Naturalem, Sistens Genera Lapidum, Plantarum et Animalium Hactenus Detecta, Caracteribus Essentialibus Donata, in Tribus Divisa, Subinde ad Leges Naturae*. Apud Wolfgangum Gerle, Prague, 506 pp.
- Shikama, T., and Y. Hasegawa. 1962. Discovery of the fossil giant salamander (*Megalobatrachus*) in Japan. *Transactions of the Proceedings of the Paleontological Society of Japan, new series* 45:197–200.
- Skutschas, P. P. 2009. Re-evaluation of *Myrbulakia* Nesov, 1981 (Lissamphibia: Caudata) and description of a new salamander genus from the Late Cretaceous of Uzbekistan. *Journal of Vertebrate Paleontology* 29:659–664.
- Swofford, D. L. 2002. PAUP*: Phylogenetic Analysis Using Parsimony (*And Other Methods), Version 4. Sinauer Associates, Sunderland, Massachusetts.
- Temminck, C. J. 1836. Coup d'Oeil sur la Fauna des îles de la Sonde et de l'Empire du Japon. Discours Préliminaire Destiné à Servir d'Introduction à la Faune du Japon. Müller, Amsterdam, 144 pp.
- Topachevskij, V. A., V. A. Nesin, I. V. Topachevskiy, and Y. A. Semenov. 1996. The oldest locality of middle Sarmatian microtheriofauna (Insectivora, Lagomorpha, Rodentia) in the Eastern Europe. *Dopovid NAN Ukrayini* 2:107–109. [Russian]
- Vangengeim, E. A., A. N. Lungu, and A. S. Tesakov. 2006. Age of the Vallesian lower boundary (Continental Miocene of Europe). *Stratigraphy and Geological Correlation* 14:655–667.
- Venczel, M. 1999. Land salamanders of the family Hynobiidae from the Neogene and Quaternary of Europe. *Amphibia-Reptilia* 20:401–412.
- Vitt, L. J., and J. P. Caldwell. 2009. *Herpetology: An Introductory Biology of Amphibians and Reptiles*, third edition. Academic Press and Elsevier, London, xiv + 697 pp.
- Westphal, F. 1958. Die Tertiären und Rezenten Eurasasiatischen Riesen-salamander (Genus *Andrias*, Urodela, Amphibia). *Palaeontographica, Abteilung A* 110:20–92.
- Zerova, G. A. 1985. Preliminary results on middle Sarmatian herpetofauna of Ukraine; pp. 78–79 in I. Darevsky (ed.), *Abstract Book of 6th All Soviet Herpetological Conference*. Nauka, Tashkent, 18–20 September 1985. [Russian]
- Zhang, P., Y.-Q. Chen, H. Zhou, Y.-F. Liu, X.-L. Wang, T. J. Papenfuss, D. B. Wake, and L.-H. Qu. 2006. Phylogeny, evolution, and biogeography of Asiatic Salamanders (Hynobiidae). *Proceedings of the National Academy Sciences of the United States of America* 103:7360–7365.

Submitted December 27, 2011; revisions received August 5, 2012; accepted August 10, 2012.

Handling editor: Jason Anderson.

APPENDIX 1. List of osteological characters used in the phylogenetic analysis.

Dentary

- (1) Shape of symphysis in cross-section: round or oval (0); elongated elliptical (1).
- (2) Triangular ventral space between the dentaries: large (0); small (1) (relationship between large and small $\sim 1.5:1$).
- (3) Sculpture of the dermal ossification on labial side of dentary: smooth or slightly wrinkled (0); rugose to pustular and pointed (1).
- (4) Lingual crista on dentary: absent (0); present (1).
- (5) Lingual surface of corpus dentalis between symphysis and beginning of Meckelian cartilage, under lamina dentalis is plain (0); has deep groove—presymphyseal sulcus (1). Comment: *Andrias scheuchzeri* has a slight ‘S’-shaped depression, which we consider to be plain (0) with respect to the scores used herein.
- (6) Ventral keel of dentary: not prolonged (0); prolonged (1).
- (7) Pars dentalis: consists of dental lamina only (0); subdivided into a dental and subdental lamina (1).
- (8) Dental shelf: plain or shallow (shallowly concave surface) (0); deep (1).
- (9) Mental foramina small, longitudinal flange not pronounced or slightly pronounced (0); mental foramina large (more than 1.5 times larger), longitudinal flange pronounced (1).
- (10) Lateral and ventral ala of symphysis: large and small (in relation $\sim 2:1$), respectively (0); small and large (in relation $\sim 1:2$), respectively (1); small and small, respectively (2).
- (11) Lateral and ventral ala of symphysis: not fused (0); fused (1).
- (12) Dentine shaft of tooth crown: present (0); reduced or absent (1). Comment: Data taken from Böttcher (1987) and Greven and Clemen (1980, 2009).

Articular

- (13) Articulation facet of articular-dentary: not pronounced (0); pronounced (1).
- (14) Labioventral facet of articular: narrow and relatively rough (0); broad and sculptured with prominent pits and ridges (1).
- (15) Articular condyle: elongated (0); short (1) ($<1.5:1$ relationship).
- (16) Articular condyle: broad (0); narrow (1) ($<1.5:1$ relationship).

Coronoid

- (17) Coronoid process: narrow (0); broad (1) ($<1:1.5$ relationship).
- (18) Coronoid process: long (0); short (1) ($<1.5:1$ relationship).

Occipital

- (19) Pericondylar facet of occipital: absent or fragmentarily preserved (0); present (1).

Squamosal

- (20) Squamosal: not robust (0); robust (1).
- (21) Eminentia dorsalis: absent (0); present (1).
- (22) Paries posterior: low (lower than paries anterior) (0); high (higher than paries anterior) (1).
- (23) Paries posterior: extends parallel and ventral to the paries dorsalis (0); extends along paries dorsal with an obtuse angle (1).

Femur

- (24) Femoral crest: short (terminates at the mid-diaphyseal position) (0); long (terminates at the lateral wall of trochlear groove) (1).

Vertebrae

- (25) Prezygapophysis and the facies articularis prezygapophysis: extremely elongated ellipse (0); round or slightly elongated (1).
- (26) Interzygapophyseal ridge, running between pre- and postzygapophysis: absent or poorly developed (0); well developed and builds lamella above transverse process (1).
- (27) Beginning of hemal process: lamella like (0); oval (1).
- (28) Hemal processes positioned: at the middle part of vertebra centrum (0); at the posterior portion of vertebral centrum (1).
- (29) Arterial canal in caudal vertebrae: narrow, with small foramen (0); broad, with large foramen (1).

Other Characters

- (30) Terminal phalanges: robust, without bulbous tips (0); slender, with bulbous tip (1).
- (31) Degree of ossification of the dentary: high (bone compactness value >0.8) (0); low (bone compactness >0.8) (1). Comment: The bone compactness value of *Onychodactylus fischeri* in Laurin et al. (2004) is given for the femur. However, the compactness value of the femur is slightly lower than that of *Andrias japonicus* and *Cryptobranchus alleganiensis*. So, we consider the value for the dentary of *Onychodactylus fischeri* to be more than 0.8.
- (32) Trunk ribs: bicapitate (0); unicapitate (1). Comment: The hynobiids were reported to have unicapitate ribs (Duellman and Trueb, 1994). This character was considered as a derived character state of the suborder Cryptobranchoidea (Cryptobranchidae + Hynobiidae) (Duellman and Trueb, 1994). However, there are several species of hynobiids both Recent (*Onychodactylus japonicus*, see Okajima, 1908:fig. 6e–j, table 13; *Onychodactylus fischeri*, GPIT/RE/7331; *Ranodon sibiricus*, see Kuzmin and Thiesmeier, 2001:fig. 35) and fossil (*Parahynobius kordosi*, *Parahynobius betfianus*, cf. *Parahynobius*, see Venczel, 1999:figs. 1, 3, 4; *Ranodon* cf. *sibiricus*, see Averianov and Tjutkova, 1995:figs. 3, 4; *Salamandrella* sp., GPIT unnumbered specimen), which show bicapitate ribs, as well as two articulation surfaces on the distal end of the transverse processes of the trunk vertebrae. We did not find any hynobiid species that show unicapitate ribs like those reported by Duellman and Trueb (1994).
- (33) Adult body size: small (<1 m) (0); large (>1 m) (1).
- (34) Parietal and squamosal: partial or not connected (0); completely connected (1).
- (35) Processus prefrontalis of maxillae: absent (0); present (1).
- (36) Vomerine dentition: curved row parallel to the maxillary and premaxillary teeth, the tooth row lies anteriorly on the vomer (0); vomerine dentition pattern is transverse and does not parallel the maxillary and premaxillary teeth, the tooth row lies posteriorly on the vomer (1). Altered from Duellman and Trueb (1994:464).
- (37) Gill slits: absent (0); present (1).
- (38) Hyobranchial apparatus: includes ossified ceratobranchial 2 and hyobranchial 2 (0); includes distal part of ceratohyal, ceratobranchial 2, and hyobranchial 2 (1).
- (39) Number of bones surrounding external naris: four bones (frontal, nasal, maxilla, and premaxilla) (0); three bones (nasal, maxilla, and premaxilla) (1).

APPENDIX 2. Character-taxon matrix used for phylogenetic analysis. ‘?’ denotes non-preservation and ‘-’ is a non-applicable character state.

<i>An. japonicus</i>	0 0 0 0 0 0 0 1 0 2 1 1 1 0 0 1 0 0 0 0 0 0 0 0 1 0 0 0 0 0 0 1 1 1 0 0 0 0 1
<i>An. davidianus</i>	0 0 0 0 0 0 0 1 0 1 1 1 1 0 0 1 0 0 0 0 0 0 0 0 1 0 0 0 0 0 0 1 1 1 1 0 0 0 1
<i>An. scheuchzeri</i>	0 0 0 0 0 0 0 1 0 0 0 1 1 1 0 0 1 1 1 1 0 0 0 0 0 0 1 0 0 0 ? 0 0 1 1 1 0 0 0 1
<i>U. hypsognathus</i>	1 1 1 1 0 1 1 0 1 ? ? ? 0 1 0 0 1 0 1 1 1 1 1 0 0 0 1 1 1 1 1 1 1 ? ? ? ?
<i>Z. beliajevae</i>	0 0 0 0 1 0 0 1 0 1 0 ? 1 0 1 1 0 0 0 0 0 ? ? 0 1 0 ? ? ? ? 0 1 1 1 1 0 ? ? ?
<i>Av. exsecratus</i>	0 0 0 0 1 0 0 1 0 0 0 ? ? ? ? ? 0 ? ? ? ? 1 1 1 ? 0 ? ? 0 1 1 1 ? ? ? ?
<i>C. alleganiensis</i>	0 0 0 0 0 0 0 1 0 1 1 0 1 0 0 1 0 0 0 0 0 0 0 0 1 0 0 0 0 0 0 1 1 1 0 0 1 1 0
‘C.’ saskatchewanensis	1 1 0 ? 1 0 0 0 0 0 0 ? ? ? ? ? ? ? ? ? ? ? ? ? ? ? ? ? ? 1 ? ? ? ? ?
<i>O. fischeri</i>	0 - 0 0 0 0 0 0 0 - - - 0 0 - 0 0 0 0 0 0 0 - - 0 0 0 0 0 0 0 ? 0 0 0 0 1 0 0 0